

# Geological Map of the Upper Laja River Basin, Guanajuato, Mexico<sup>☆</sup>

## Mapa geológico de la Cuenca Alta del Río Laja, Guanajuato, México

Beatriz Coral Beltrán Martínez<sup>a</sup>, Isidro Loza Aguirre<sup>b</sup>, Yanmei Li<sup>b</sup>, Raúl Miranda Avilés<sup>b</sup>, Ángel F. Nieto Samaniego<sup>c</sup>, Edgar Angeles Moreno<sup>b</sup>, Pooja Vinod Kshirsagar<sup>b</sup>, María Jesús Puy y Alquiza<sup>b</sup>, Jesús Horacio Hernández Anguiano<sup>d</sup>

<sup>a</sup>Maestría en Ciencias del Agua, División de Ingenierías, Universidad de Guanajuato, 36000, Guanajuato, Gto., México

<sup>b</sup>Departamento de Ingeniería en Minas, Metalurgia y Geología, División de Ingenierías, Campus Guanajuato, Universidad de Guanajuato, 36020, Guanajuato, Gto., México

<sup>c</sup>Centro de Geociencias, Universidad Nacional Autónoma de México, Campus Juriquilla, Querétaro, 76230, México

<sup>d</sup>Departamento de Ingeniería Geomática e Hidráulica, División de Ingenierías, Campus Guanajuato, Universidad de Guanajuato, 36000, Guanajuato, Gto., México

### Abstract

A new geological map of the Upper Laja River Basin at 1:200,000 scale is presented, covering an area of ~11,600 km<sup>2</sup> in the northern part of Guanajuato. This map was edited based on local and regional geological studies available in the literature, photo interpretations, field verification of contacts and faults and structural data acquisition. The main objective of this map is to provide a regional geological framework for future local geological and hydrological studies in the region. It displays the geology of the basin, divided into seven chronostratigraphic groups, as well as the main faults that shape the basin. In contribution to the geological knowledge of the area, five new U-Pb ages are presented, obtained from samples collected at the eastern and western edges of the basin.

**Keywords:** Upper Laja River Basin, Geology, Geochronology.

### Resumen

Se presenta un nuevo mapa geológico de la Cuenca Alta del Río Laja (CARL) a escala 1:200,000 que abarca un área de ~11,600 km<sup>2</sup> en el norte de Guanajuato. Este mapa fue editado a partir de estudios geológicos locales y regionales disponibles en la literatura, fotointerpretaciones y observaciones de contactos, fallas y datos estructurales en campo. El objetivo principal de este mapa es proporcionar una base geológica regional para futuros estudios geológicos e hidrológicos locales en la región. En él se muestra la geología de la cuenca, dividida en siete grupos cronoestratigráficos, así como las principales fallas que forman la cuenca. En contribución al conocimiento geológico de la zona se presentan cinco nuevas edades U-Pb obtenidas de muestras recolectadas en los bordes oriental y occidental de la cuenca.

**Palabras clave:** Cuenca Alta del Río Laja, Geología, Geocronología.

### 1. Introduction

The Upper Laja River Basin (ULRB) is part of the Lerma-Chapala Basin, which belongs to the hydrological region RH12

Lerma-Santiago (Figure 1a). Physiographically, the ULRB is in the Mesa Central province, and to the south, it encompasses a small part of the Trans-Mexican Volcanic Belt (Figure 1b). Geographically, it is situated in the northeast of the state of Guanajuato, covering the municipalities of Dolores Hidalgo, San Miguel de Allende, San Felipe, San Diego de la Unión, San Luis de la Paz, San José Iturbide, Doctor Mora, and Guanajuato (Figure 1c).

For several decades, geological studies have been carried out in the ULRB, providing valuable geochronological, stratigraphic, and tectonic information about the area (Alaniz-Alvarez

<sup>☆</sup>© B. C. Beltrán Martínez, I. Loza Aguirre, Y. Li, R. Miranda Avilés, Á. F. Nieto Samaniego, E. Ángeles Moreno, P. Vinod Kshirsagar, M. J. Puy y Alquiza and J. H. Hernández Anguiano. This is an Open Access article distributed under the terms of the Creative Commons Attribution License (<https://creativecommons.org/licenses/by-nc-sa/4.0/>), which permits non-commercial sharing of the work and adaptions, provided the original work is properly cited and the new creations are licensed under identical terms.

\*E-mail address: beatriz\_bmtz@outlook.com

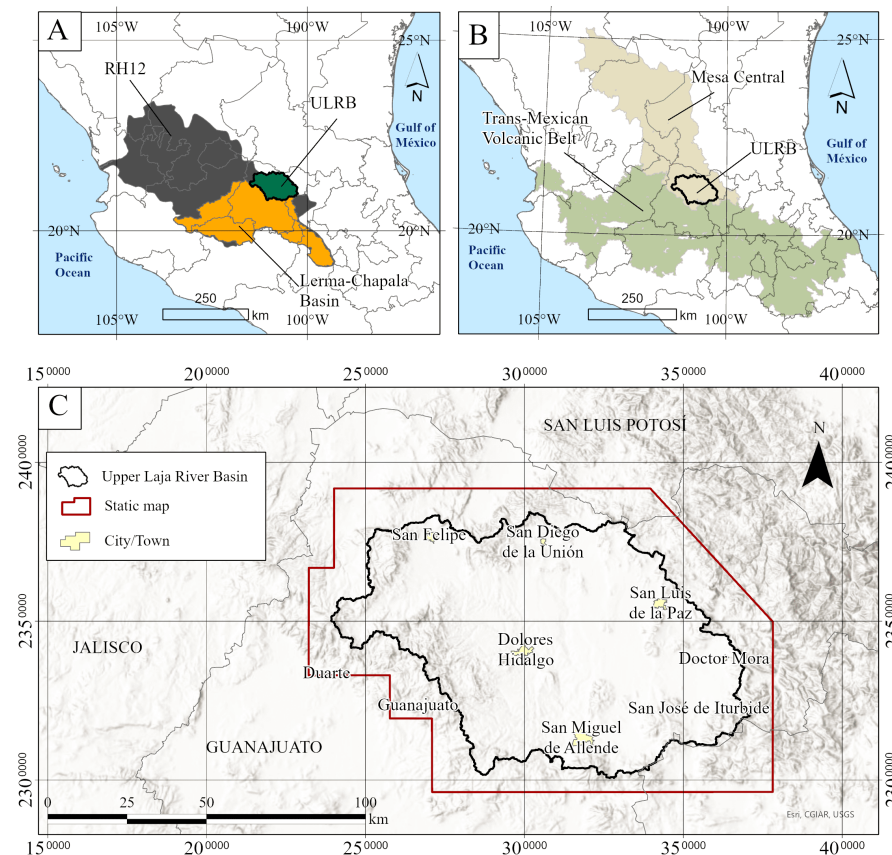


Figure 1. A) Hydrological location map of the ULRB. B) Physiographic location map of the ULRB. C) Geographic location map of the ULRB, with a red polygon showing the area covering by the geologic map of this work. / Figura 1. A) Mapa de ubicación hidrológica de la CARL. B) Mapa de ubicación fisiográfica de la CARL. C) Mapa de ubicación geográfica de la CARL, con un polígono rojo se muestra el área que abarca el mapa geológico de este trabajo.

et al., 2001; Nieto-Samaniego et al., 2012; Ángeles-Moreno, 2018; Del Río-Varela et al., 2020; Del Pilar-Martínez et al., 2021). These investigations have provided insight into the geological evolution of the region. However, it is important to remember that these studies only partially covered the basin, which implies that the available information may not fully represent the entire area. Additionally, the lithological limits and geological formations mentioned in previous maps sometimes differ from one map to another, perhaps due to the complexity of the area's geology and limitations in the compilation.

In this paper, we present a geological map at 1:200,000 scale, edited to integrate the existing information. The map was complemented with field observations, photo interpretations, and five new U-Pb isotopic ages. It shows the dominant fault systems that constitute the basin, as well as the main groups of metamorphic, igneous, and sedimentary rocks in the ULRB, organized based on their approximate ages. It is expected that this map would be a valuable resource for future research and studies in the region, considering the geological and hydrogeological importance of the basin, which encompasses several “critical aquifers”.

## 2. Methods

### 2.1. Geological map

The ULRB geological map covers an area of ~11,600 km<sup>2</sup> and is based on previous geological and structural studies, including 18 geological charts at 1:50,000 scale published by the Servicio Geológico Mexicano (SGM) (Table 1), as well as other geological data integrated from Alaniz-Álvarez et al.(2001), Alaniz-Álvarez et al.(2002), Del Río-Varela et al.(2020) and Castro-Aceves(2020) (Figure 2).

The proposed stratigraphic column of the ULRB was edited based on the main volcanic and sedimentary events, which were constrained according to the geochronology and nomenclature of the formations described in the above-mentioned literature.

Geological fieldwork was conducted throughout the entire basin and its surroundings to obtain sufficient lithological and structural data. Particularly, significant attention was given to the mountain ranges bordering the basin, as they constitute the primary outcrop sites of the rock units that make up the basin's stratigraphic column.

Table 1. List of 1: 50,000 scale geologic maps published by the SGM used in this work / Tabla 1. Lista de los mapas geológicos a escala 1: 50,000 publicados por el SGM utilizados en este trabajo

Key	Name	Authors
F14-C22	Sierra de Jacales	Lemos-Bustos and Flores-Salas (2020)
F14-C32	Ibarra	Soto-Araiza and Arredondo (2005)
F14-C42	Nuevo Valle de Moreno	Alvarado-Méndez and Rodríguez-Trejo (1999)
F14-C23	Presa San Bartolo	Gómez-Ordaz et al. (2016)
F14-C33	San Felipe	Bustos-Gutiérrez and Romo-Ramírez (2005)
F14-C43	Guanajuato	Alvarado-Méndez Héctor et al. (1998)
F14-C53	Aldama	López-Ojeda et al. (2002)
F14-C24	Melchor	Gómez-Ordaz and Ávila-Ramos (2017b)
F14-C34	San Diego de la Unión	Procesos Analíticos Informáticos S.A. de C.V. (2008a)
F14-C44	Dolores Hidalgo	Pérez-Vargas et al. (1996)
F14-C54	San Miguel de Allende	Nieto-Samaniego et al. (1999b)
F14-C25	Tierra Nueva	Sociedad Exploradora Minera S.A. de C.V. (1999b)
F14-C35	San Luis de la Paz	Procesos Analíticos Informáticos S.A. de C.V. (2008b)
F14-C45	Mineral de Pozos	Reyes-Reyes and Castro-Luna (1998)
F14-C55	Buenavista	Gómez-Ordaz and Ávila-Ramos (2017a)
F14-C36	Xichú	Servicios Geológicos Mineros S.A. de C.V. (2001)
F14-C46	Doctor Mora	Sociedad Exploradora Minera S.A. de C.V. (1999a)
F14-C56	Colón	Arredondo-Mendoza and García-Ortíz (2007)

The geological map was digitized using ArcMap 10.5 software. Lithological boundaries and some faults were redrawn based on geochronological data, lithological descriptions, field observations, photogeological interpretations of Google Earth satellite images, and digital elevation models edited by the Instituto Nacional de Estadística y Geografía (INEGI).

The map's geochronologic accuracy is supported by 118 isotopic ages, mainly obtained from the compilations made by Alanís-Ruiz (2002) and Del Pilar-Martínez et al. (2021).

## 2.2. U-Pb geochronology

Five samples with keys SRD-03, SRD-23, SRD-26, SLTN-05, and SLTN-16 were dated. The first three samples were collected in the Sierra de Guanajuato, on the western boundary of the ULRB. The remaining two samples were collected in the north of San Luis de la Paz, on the northeastern boundary of the basin.

The zircon samples were analyzed using the LA-ICPMS technique at the Laboratorio de Estudios Isotópicos of the Centro de Geociencias in the Universidad Nacional Autónoma de México, following the methodology outlined in Solari et al. (2018).

Concordance and weighted means plots were constructed using Isoplot v. 4.1 (Ludwig, 2008).

## 3. Stratigraphy of the Upper Laja River Basin

The geological units outcropping in the ULRB were divided into three complexes: (1) Mesozoic metavolcanic and metasedimentary rocks, (2) Cenozoic volcanic rocks and sedimentary deposits, and (3) Miocene-Holocene sedimentary cover.

In this work, Cenozoic rocks were categorized into five chronostratigraphic groups according to their isotopic ages: (1) lower Eocene sedimentary deposits and felsic volcanic rocks, (2) upper Eocene-lower Oligocene volcanic rocks, (3) middle Oligocene felsic rocks, (4) upper Oligocene-lower Miocene sedimentary deposits and felsic rocks, (5) Miocene intermediate and mafic rocks.

### 3.1. Mesozoic

Mesozoic rocks constitute the basement of the ULRB and exhibit a diverse composition. The lowermost part of this sequence (key JKIMV on Plate 1) comprises marine volcanic rocks, massive lava flows, pillow lavas, diorites, and granitoid dikes. This group includes the San Juan de Otates ultramafic-mafic complex (Ortiz-Hernández et al., 1992), the La Luz Basaltic Unit (Monod et al., 1990; Ortiz-Hernández et al., 1992), the Santa Ana Philonian Complex (Ortiz-Hernández et al., 1992), the Cerro Pelón tonalite (Monod et al., 1990) and the Tuna Mansa diorite (Ortiz-Hernández et al., 1992).

The upper part comprises marine sedimentary rocks such as sandstones, shales, and carbonate sediments (key KiMCz-Ar on Plate 1), that includes the Arperos Formation (Chiodi et al., 1988; Monod et al., 1990), Esperanza Formation (Echegoyen-Sánchez, 1978; Ortiz-Hernández et al., 1992), and Perlita Limestone (Quintero-Legorreta, 1992) (see ages in Figure 3). It is noteworthy that the entire Mesozoic sequence has undergone low-grade metamorphism (Alaniz-Alvarez et al., 2001; Alanis-Ruiz, 2002).

The main Mesozoic outcrops are located in the Sierra de Guanajuato, Sierra de los Cuarzos, and Sierra de Pozos. Minor outcrops have been identified in Sierra de Santa Barbara, south-

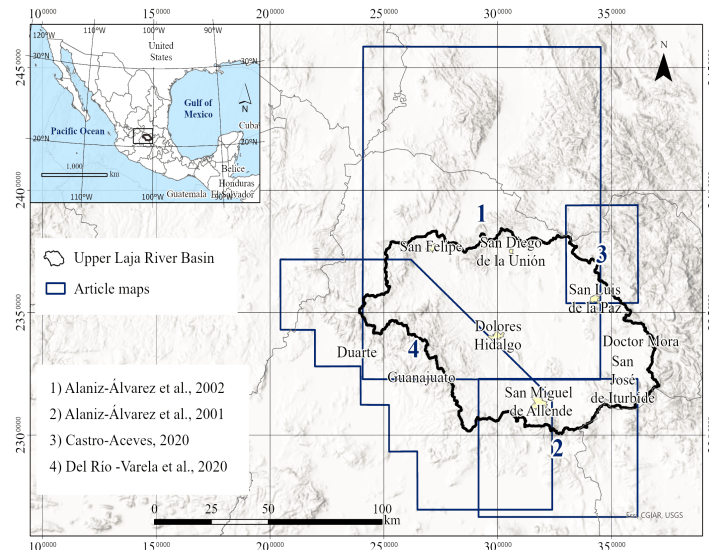


Figure 2. Location of previously published local geological maps. The blue polygons represent the local maps used as references for this work. / Figura 2. Ubicación de los mapas geológicos locales publicados anteriormente. En polígonos azules se muestran los mapas locales usados como referencia para este trabajo.

east of Sierra de Codornices, north of San Miguel de Allende, and northeast of Doctor Mora (Figure 3 and Plate 1).

### 3.2. Cenozoic

#### 3.2.1. Lower Eocene

The Cenozoic deposits of the ULRB are composed of volcanic-plutonic and sedimentary rocks, originated by several magmatic pulses. The complex formation begins in the Lower Eocene with the emplacement of the Comanja Granite (Echegoyen-Sánchez et al., 1970; key TeGr on Plate 1), that outcrops in the Sierra de Guanajuato following an NW-SE orientation (Figure 4 and Plate 1); continuing with a brief episode of lava emissions, as well as small subvolcanic intrusive bodies, such as the Laborcita Rhyolite (Angeles-Moreno, 2018), Palo Blanco Ignimbrite and Duarte Sill (Angeles-Moreno, 2018). These events were contemporaneous with the sedimentation of the Guanajuato Conglomerate (Echegoyen-Sánchez et al., 1970) and Duarte Conglomerate (Martínez-Reyes, 1992; key TeRCgp on Plate 1), with outcrops in the Sierra de Guanajuato, Sierra de Codornices and Sierra de Santa Barbara (Figure 4 and Plate 1).

In the Sierra de Guanajuato, these continental conglomerates discordantly overlie Mesozoic rocks. The Duarte Sill outcropping near the margins of the Duarte Dam, was previously included in the Duarte Conglomerate, but Angeles-Moreno (2018) makes a distinction between them. The Laborcita Rhyolite is interbedded with the Duarte Conglomerate and underlies the Palo Blanco Ignimbrite (Angeles-Moreno, 2018).

#### 3.2.2. Upper Eocene - lower Oligocene

During the upper Eocene-lower Oligocene, an intense and prolonged period of effusive and explosive volcanism took place,

producing volcanic rocks of rhyolitic composition and associated tuffs (key TOR on Plate 1), basalts and andesites (key ToA on Plate 1). These volcanic formations crops out along the basin rim and in small areas of its interior (Figure 5 and Plate 1).

The rhyolites and tuffs include: the Losero Formation (Echegoyen-Sánchez et al., 1970) and Bufo Formation (Echegoyen-Sánchez et al., 1970; Davis et al., 2009) of Guanajuato Volcanic Group (Nieto-Samaniego et al., 2015) overlying the Guanajuato Conglomerate; the Alfaro Ignimbrite (Ángeles-Moreno, 2018) that overlies Eocene rocks in angular unconformity (Ángeles-Moreno, 2018); the Chichíndaro Rhyolite (Echegoyen-Sánchez et al., 1970) that appears overlying the El Cedro Formation and underlying the Cañada La Virgen Ignimbrite in the Guanajuato Mining District (Angeles-Moreno, 2018); the San Miguelito Rhyolite (Labarthe-Hernández and Tristán-González, 1978), and Cañada La Virgen Tuff (Cerca-Martínez et al., 2000) that overlies Oligocene andesites and underlies discordantly the Cañada La Virgen Ignimbrite in the locality of Cañada La Virgen.

The basalts and andesites, grouped in the Cedro Formation of the Guanajuato Volcanic Group, crop out in the Sierra de Guanajuato, Sierra de Codornices, Sierra del Cuarzo, Sierra de Santa Barbara, and northeast of San Luis de la Paz (Figure 5 and Plate 1)

#### 3.2.3. Middle Oligocene

During the middle Oligocene, volcanic rocks (key TochIg on Plate 1), crop out mainly in the Sierra de Santa Bárbara, Sierra de Guanajuato, and Sierra de Codornices (Figure 6 and Plate 1).

These volcanic rocks include the Cañada La Virgen Ignimbrite (Nieto-Samaniego et al., 1996) which is discordantly covered by the Santa Catarina Conglomerate and San Nicolás

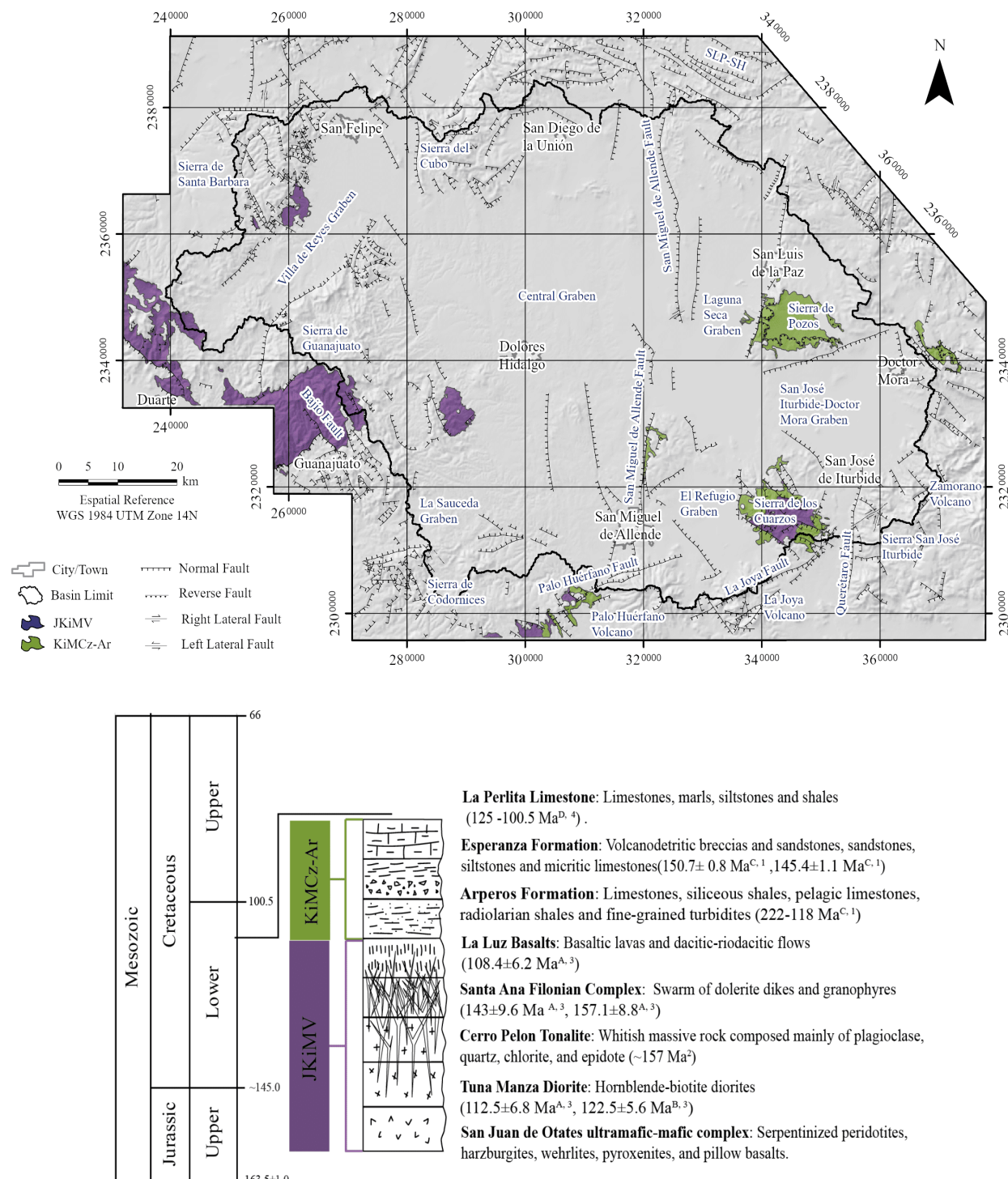


Figure 3. Location of Mesozoic outcrops, and Mesozoic stratigraphic column of the ULRB. Formations included in each chronostratigraphic group are shown according to their reported ages. Dating method: K/Ar in whole rock <sup>A</sup>, K/Ar in amphibole <sup>B</sup>, U-Pb in zircon <sup>C</sup>, Fossil fauna <sup>D</sup>. Source: Martini et al. (2011)<sup>1</sup>, Monod et al. (1990)<sup>2</sup>, Ortiz-Hernández et al. (1992)<sup>3</sup>, Chiodi et al. (1988)<sup>4</sup> / Figura 3. Ubicación de los afloramientos mesozoicos y columna estratigráfica Mesozoica de la CARL. Se muestran las formaciones que incluye cada grupo crono estratigráfico de acuerdo con sus edades reportadas. Método de datación: K/Ar en roca entera <sup>A</sup>, K/Ar en anfibol <sup>B</sup>, U-Pb en zircón <sup>C</sup>, Fauna fósil <sup>D</sup>. Fuente: Martini et al. (2011)<sup>1</sup>, Monod et al. (1990)<sup>2</sup>, Ortiz-Hernández et al. (1992)<sup>3</sup>, Chiodi et al. (1988)<sup>4</sup>

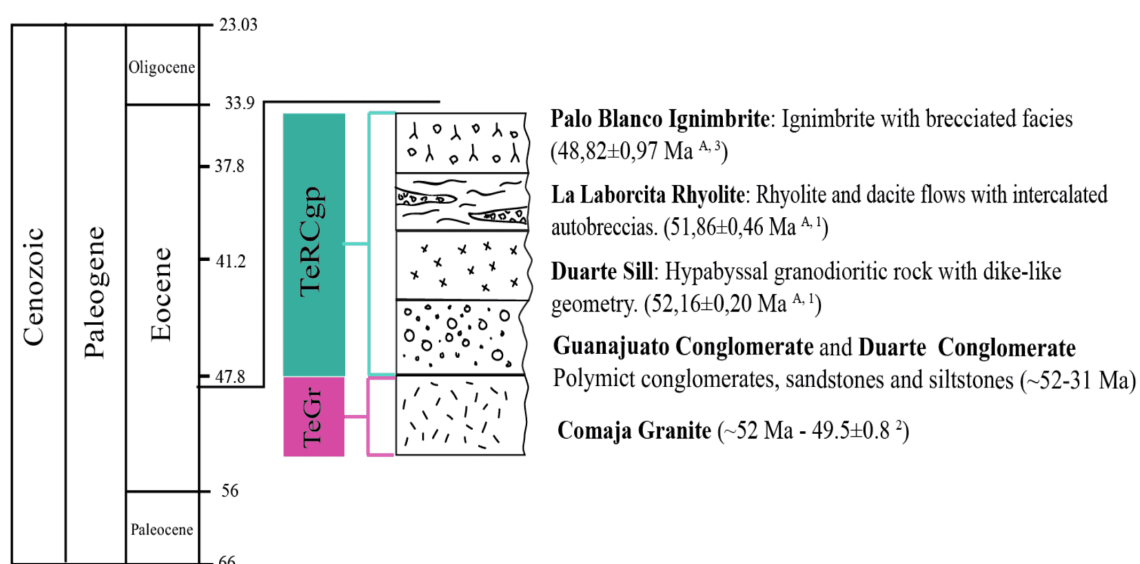
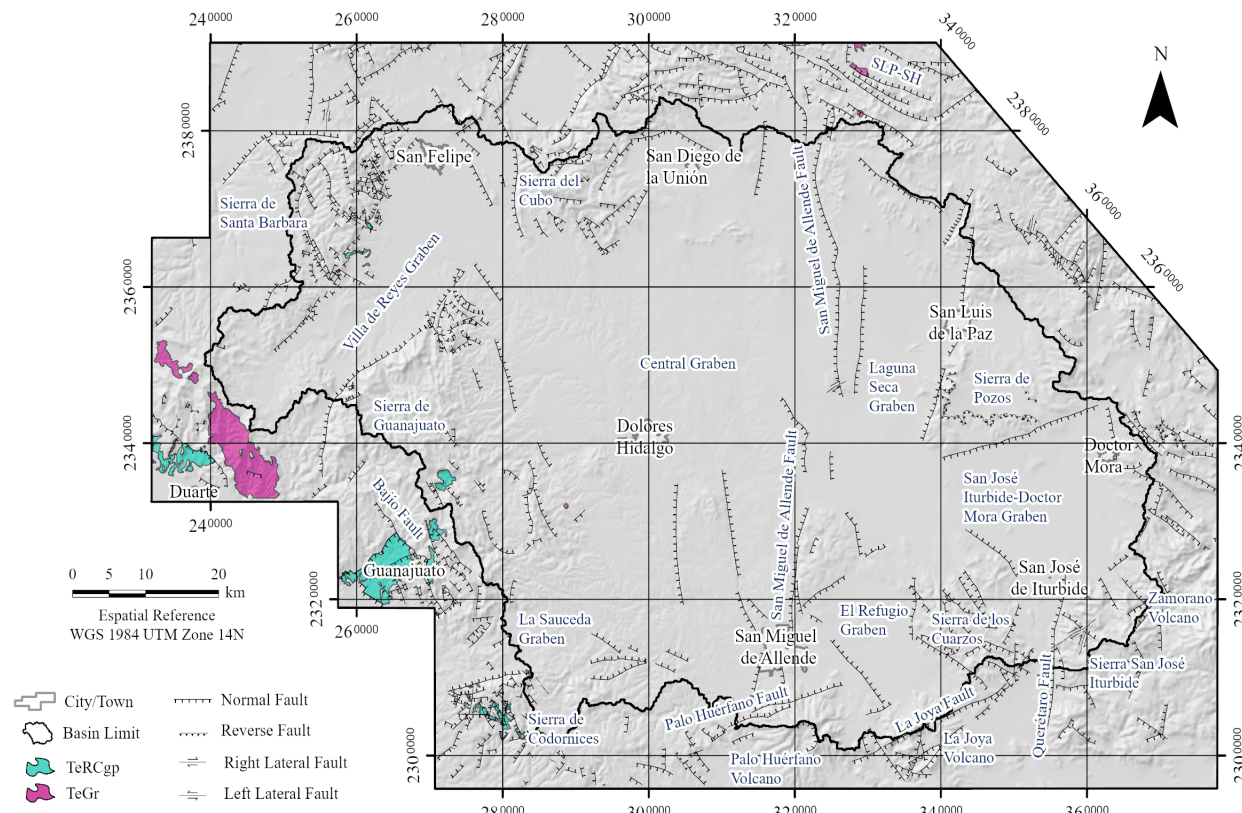


Figure 4. Location of lower Eocene outcrops and lower Eocene stratigraphic column of the ULRB. Formations included in each chronostratigraphic group are shown according to their reported ages. Dating method: U-Pb in zircon<sup>A</sup>. Source: Ángeles-Moreno, (2018)<sup>1</sup>, Nieto-Samaniego et al. (2015)<sup>2</sup>, Ruiz-González, (2015)<sup>3</sup> / Figura 4. Ubicación de los afloramientos del Eoceno inferior y columna estratigráfica del Eoceno inferior de la CARL. Se muestran las formaciones que incluye cada grupo cronoestratigráfico de acuerdo con sus edades reportadas. Método de datación: U-Pb en zircón<sup>A</sup>. Fuente: Ángeles-Moreno, (2018)<sup>1</sup>, Nieto-Samaniego et al. (2015)<sup>2</sup>, Ruiz-González, (2015)<sup>3</sup>

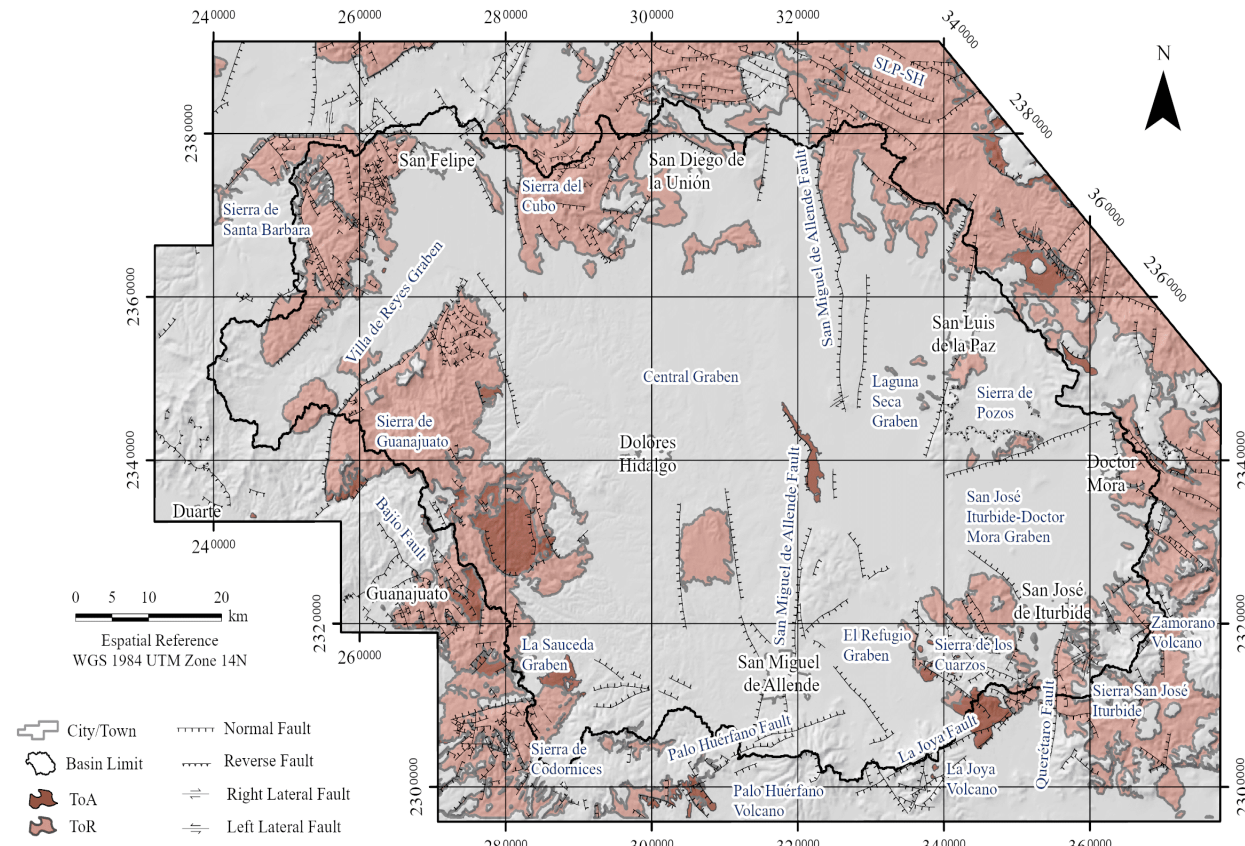


Figure 5. Location of upper Eocene-lower Oligocene outcrops and upper Eocene-lower Oligocene stratigraphic column of the ULRB. For mations included in each chronostratigraphic group are shown according to their reported ages. Dating method: K/Ar in whole rock <sup>A</sup>, K/Ar, in rock matrix <sup>B</sup>, K/Ar in sanidine <sup>C</sup>, Ar/Ar in sanidine <sup>D</sup>, U-Pb in zircon <sup>E</sup>. Source: Ángeles-Moreno, (2018)<sup>1</sup>, Cerca-Martínez et al. (2000)<sup>2</sup>, Labarthe-Hernández et al. (1982)<sup>3</sup>, Nieto-Samaniego et al. (2015)<sup>4</sup>, Nieto-Samaniego et al. (1996)<sup>5</sup> / Figura 5. Ubicación de los afloramientos del Eoceno superior-Oligoceno inferior y columna estratigráfica del Eoceno superior-Oligoceno inferior de la CARL. Se muestran las formaciones que incluye cada grupo crono estratigráfico de acuerdo con sus edades reportadas. Método de datación: K/Ar en roca entera <sup>A</sup>, K/Ar, en matriz <sup>B</sup>, K/Ar en sanidino <sup>C</sup>, Ar/Ar en sanidino <sup>D</sup>, U-Pb en zircón <sup>E</sup>. Fuente: Ángeles-Moreno, (2018)<sup>1</sup>, Cerca-Martínez et al. (2000)<sup>2</sup>, Labarthe-Hernández et al. (1982)<sup>3</sup>, Nieto-Samaniego et al. (2015)<sup>4</sup>, Nieto-Samaniego et al. (1996)<sup>5</sup>

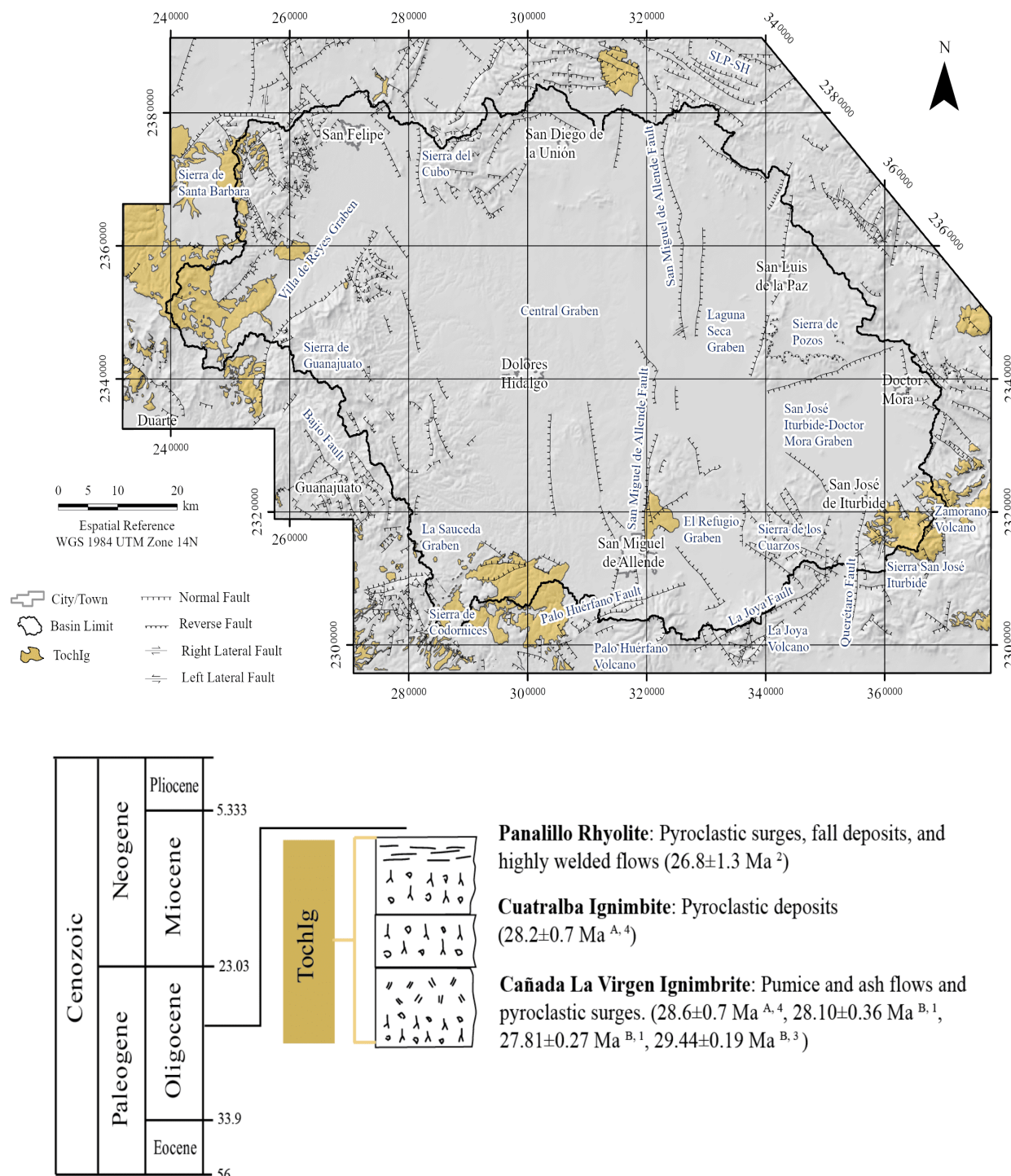
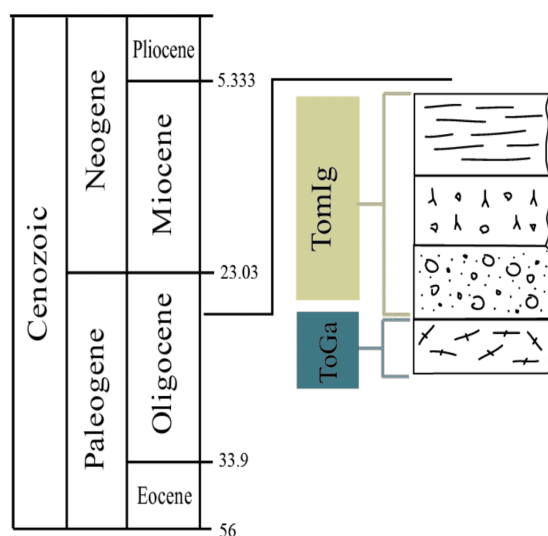
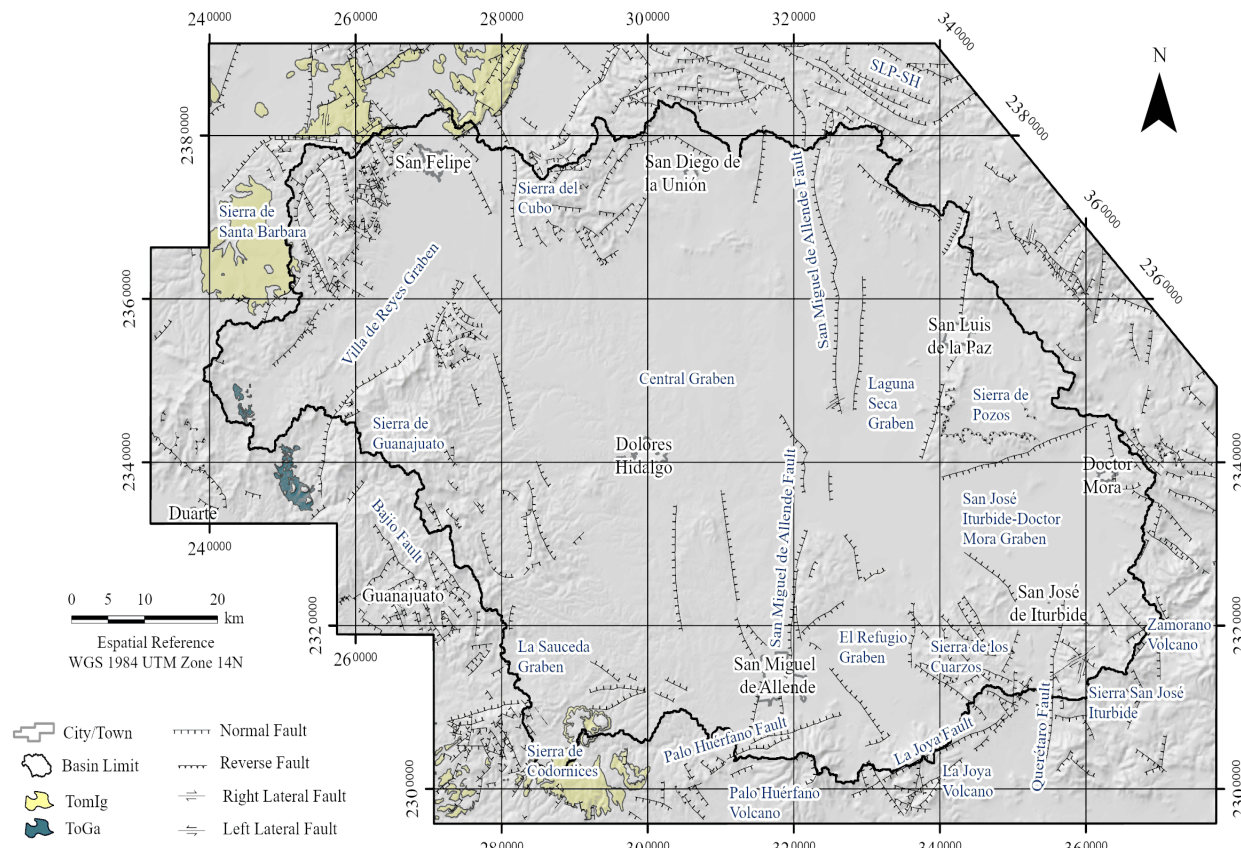


Figure 6. Location of middle Oligocene outcrops and middle Oligocene stratigraphic column of the ULRB. Formations included in each chronostratigraphic group are shown according to their reported ages. Dating method: K/Ar in sanidine<sup>A</sup>, U-Pb in zircon<sup>B</sup>. Source: Ángeles-Moreno, (2018)<sup>1</sup>, Labarthe-Hernández et al. (1982)<sup>2</sup>, Nieto-Samaniego et al. (2015)<sup>3</sup>, Nieto-Samaniego et al. (1996)<sup>4</sup> / Figura 6. Ubicación de los afloramientos del Oligoceno medio y columna estratigráfica del Oligoceno medio de la CARL. Se muestran las formaciones que incluye cada grupo crono estratigráfico de acuerdo con sus edades reportadas. Método de datación: K/Ar en sanidino<sup>A</sup>, U-Pb en zircón<sup>B</sup>. Fuente: Ángeles-Moreno (2018)<sup>1</sup>, Labarthe-Hernández et al. (1982)<sup>2</sup>, Nieto-Samaniego et al. (2015)<sup>3</sup>, Nieto-Samaniego et al. (1996)<sup>4</sup>



**Media Luna Ignimbrite** Highly welded pyroclastic flows ( $22.95 \pm 0.15$  Ma <sup>B, 2</sup>,  $23.96 \pm 0.20$  Ma <sup>B, 1</sup>,  $23.86 \pm 0.17$  Ma <sup>B, 1</sup>,  $22.6 \pm 0.4$  Ma <sup>A, 1</sup>)

**San Nicolas Ignimbrite:** Pyroclastic flows ( $24.8 \pm 0.6$  Ma <sup>A, 4</sup>,  $24.7 \pm 1.1$  Ma <sup>A, 3</sup>,  $23.98 \pm 0.15$  Ma <sup>B, 1</sup>)

**Santa Catarina Conglomerate:** Gravels, sands and tuffaceous material

**Arperos Gabro**

Figure 7. Location of upper Oligocene-lower Miocene outcrops and upper Oligocene-lower Miocene stratigraphic column of the ULRB. Formations included in each chronostratigraphic group are shown according to their reported ages. Dating method: K/Ar in sanidine <sup>A</sup>, U-Pb in zircon <sup>B</sup>. Source: Ángeles-Moreno (2018)  
<sup>1</sup>, Botero-Santa et al. (2015)<sup>2</sup>, Nieto-Samaniego et al. (2012)<sup>3</sup>, Nieto-Samaniego et al. (1996)<sup>4</sup> / Figura 7. Ubicación de los afloramientos del Oligoceno superior-Mioceno inferior y columna estratigráfica del Oligoceno superior-Mioceno inferior de la CARL. Se muestran las formaciones que incluye cada grupo cronoestratigráfico de acuerdo con sus edades reportadas. Método de datación: K/Ar en sanidino <sup>A</sup>, U-Pb en zircón <sup>B</sup>. Fuente: Ángeles-Moreno (2018)<sup>1</sup>, Botero-Santa et al. (2015)<sup>2</sup>, Nieto-Samaniego et al. (2012)<sup>3</sup>, Nieto-Samaniego et al. (1996)<sup>4</sup>

Ignimbrite (Angeles-Moreno, 2018); the Cuatralba Ignimbrite (Quintero-Legorreta, 1992; Martínez-Reyes, 1992) that overlies discordantly the Mesozoic basement and the Comanja Granite and underlying volcanic rocks of the Miocene group (Quintero-Legorreta, 1992; Angeles-Moreno, 2018), and the Panalillo Rhyolite (Labarthe-Hernández et al., 1982) filling depressions in the north of the ULRB.

### 3.2.4. Upper Oligocene – lower Miocene

The upper Oligocene-lower Miocene is represented by volcanic and sedimentary rocks (key TomIg on Plate 1) and gabbroic intrusives (key ToGa on Plate 1), reported in Sierra de Santa Barbara and Sierra de Codornices (Figure 7 and Plate 1).

Among these rocks are:

- The Santa Catarina Conglomerate (Nieto-Samaniego et al., 1992), which crops out in the east of the Mesa San José de Allende, conformably underlies the San Nicolás Ignimbrite and overlies the Cañada La Virgen Ignimbrite in erosional unconformity (Angeles-Moreno, 2018).
- The San Nicolás Ignimbrite (Nieto-Samaniego et al., 1990) interbedded with basin-filling sediments in the La Sauceda Graben (Nieto-Samaniego, 1990). In the Sierra de Guanajuato, the San Nicolás Ignimbrite covers the Chichíndaro Rhyolite and the Santa Catarina conglomerate, although it is most found overlying Rupelian ignimbrites (Del Río Varela et al., 2020).
- The Media Luna Ignimbrite (Botero-Santa et al., 2015) which is in fault contact with the Vulcano-sedimentary Complex of Guanajuato and covers in angular discordance the Cuatralba Ignimbrite and the Duarte Conglomerate in the Ibarrilla area (Botero-Santa et al., 2015), whilst in the Duarte area is in fault contact with the Mesozoic basement and discordantly overlies the Alfaro Ignimbrite (Angeles-Moreno, 2018), the Santa Catarina Conglomerate (Nieto-Samaniego et al., 1992), and Arperos Gabbro (Tristán-González, 1986).
- The Arperos Gabbro (Tristán-González, 1986) intrudes the Cuatralba Ignimbrite and is covered by Miocene basalts (Vassallo-Morales et al., 2001).

### 3.2.5. Miocene volcanic rocks

The Miocene volcanism of the region is characterized by plateaus and volcanic cones of basaltic to andesitic compositions (key TmA-B on Plate 1). These units crop out throughout the basin, covering Mesozoic, Eocene, and Oligocene deposits. The most extensive outcrops are found in the eastern part of the basin, highlighting the deposits of La Joya, Palo Huérfano, and Zamorano volcanoes. In the western part of the basin, scarce outcrops have been reported, such as the Mesa de San José basalt (Nieto-Samaniego et al., 1992) in the southeastern Sierra de Guanajuato and the basalts of the Mesa del Obispo, to the northeast of Duarte (Figure 8 and Plate 1).

### 3.2.6. Miocene-Holocene sedimentary succession

The Miocene-Holocene sedimentary cover (the key TnAr-Cgp on Plate 1) (Figure 9 and Plate 1) is characterized by a succession of alternating conglomerates, sandstones, siltstones, marls, limestone, and flint lenses, as well as air fall tuffs and reworked pyroclastic material (Alaniz-Álvarez et al., 2001). Nieto Samaniego (1990) reported that the San Nicolás Ignimbrite is intercalated with these sediments in the Graben de la Sauceda. In the southern part of the basin, in the Laja River, gravels underlie Miocene andesites (Cerca-Martínez et al., 2000).

Ar-Ar ages of 3.3 Ma and 4.8 Ma have been reported for volcanic ash by Kowallis et al. (1998). Near San Miguel de Allende, Carranza-Castañeda et al. (1994) and Miller and Carranza (1998) collected different species of major vertebrates in silt clay facies, suggesting at least three different periods of deposition in the late Miocene, Pliocene, and Pleistocene.

## 4. New U-Pb isotopic ages

Five new U-Pb ages were obtained for zircon crystals using the LA-ICPMS method. Samples SRD-03, SRD-23, and SRD-26 were collected northeast of Guanajuato, towards the western boundary of the basin, and samples SLTN-05 and SLTN-16 were taken north of San Luis de la Paz, in the northeastern part of the basin (Plate 1).

Sample SLTN-05 is a light pink rhyolite with well-defined flow bands, quartz crystals, and micas. It is intercalated with tuffs and ignimbrites. The age of this sample was obtained from a population of twelve data points ( $n=12$ ), which yielded a weighted mean age of  $30.18 \pm 0.23$  Ma, with an MSWD (Mean Squared Weighted Deviation) equal to 5.0 (Figure 10a, b). Sample SLTN-16 is a grayish rhyolite with a phaneritic texture, containing quartz, plagioclase, and micas. It is interbedded with tuffs and ignimbrites and discordantly overlies basalts that correlate with the El Cedro Formation. The age of this sample was obtained from a population of seven data points ( $n=7$ ), which yielded a weighted mean age of  $30.96 \pm 0.80$  Ma, with an MSWD equal to 19 (Figure 10c, d).

Sample SRD-03 is a welded, brown rhyolite with a high content of quartz and feldspar. It discordantly overlies highly altered andesites, which are correlated with the El Cedro Formation. The age of this sample was obtained from a population of five data points ( $n=5$ ), which yielded a weighted mean age of  $30.21 \pm 0.69$  Ma, with an MSWD of 2.6 (Figure 11a, b). Sample SRD-23 is a welded, dark brown vitric rhyolite characterized by the presence of abundant silica precipitation in geodes. This sample also discordantly overlies highly altered andesites correlated with the El Cedro Formation. The age of this sample was obtained from a population of eight data points ( $n=8$ ) and yielded a weighted mean age of  $29.88 \pm 0.24$  Ma, with an MSWD equal to 0.94 (Figure 11c, d). Sample SRD-26 is a rhyolitic dike that intrudes andesites correlated with the El Cedro Formation. The age of this sample was obtained from a population of eleven data points ( $n=11$ ), which yielded a weighted

mean age of  $30.86 \pm 0.39$  Ma, with an MSWD of 2.8 (Figure 11e, f).

According to the ages obtained for these five samples (Table 2), they all belong to the Upper Eocene-Lower Oligocene group. These five samples' lithological characteristics, age, and stratigraphic position suggest a possible correlation with the Chichindaro rhyolite.

Table 2. Samples dated by the laser ablation inductively coupled plasma mass spectrometry (LA-ICP-MS) U/Pb method in zircon / Tabla 2. Muestras fechadas por el método de ablación láser con masas ICP (LA-ICP-MS) U/Pb en círcón

Sample key	Coordinates (14Q)	Locality	Age
	East	North	
SRD-26	276170.3	2333684.6	Guanajuato $30.86 \pm 0.39$
SRD-23	275470.3	2334558.8	Guanajuato $29.88 \pm 0.24$
SRD-03	273513.8	2333464.0	Guanajuato $30.21 \pm 0.69$
SLTN-05	343393	2371545.9	San Luis de la Paz $30.18 \pm 0.23$
SLTN-16	355657.3	2365967	San Luis de la Paz $30.96 \pm 0.8$

## 5. Main structures in the Upper Laja River Basin

The ULRB is affected by three main fault systems: N-S, NE-SW, and NW-SE (Figure 12). The N-S system is characterized by the normal faulting of the Taxco-San Miguel de Allende Fault System (Demant, 1978) and the Querétaro Fault (Alaniz-Álvarez et al., 2001). The NE-SW system is represented by the Villa de Reyes Graben (Tristán-González, 1986; Nieto-Samaniego et al., 1999a), the Palo Huérano Fault, and the La Joya Fault. The NW-SE system is represented by the Bajío Fault System (Alaniz-Álvarez et al., 2001) and the San Luis de la Paz-Salinas Hidalgo Fault System (Nieto-Samaniego et al., 1997).

Alaniz-Álvarez et al. (2001) recognize at least two phases of activity in the Taxco-San Miguel de Allende Fault System during the Oligocene and Miocene, which caused vertical displacements of up to 450 m, cutting through Mesozoic rocks, Oligocene ignimbrites, and the early lava flows of the Palo Huérano Volcano. In the study area, this fault extends from San Diego de la Unión town to the Palo Huérano Volcano.

The Querétaro Fault developed between 10 to 5.3 Ma, with a reactivation in the Quaternary (Alaniz-Álvarez et al., 2002). With a length of 61 km and a maximum displacement of 80 m (Alaniz-Álvarez et al., 2001) the Querétaro Fault juxtaposes Oligocene ignimbrites and Miocene basalts with recent sedimentary deposits in the southeast of the basin.

Within the NE-SW system, the Villa de Reyes Graben is a tectonic basin with a displacement greater than 500 m, formed

between 26-28 Ma (Labarthe-Hernández et al., 1982; Tristán-González, 1986; Nieto-Samaniego et al., 1997; Aranda-Gómez et al., 2000). The study area covers only the southern portion of Villa de Reyes Graben, from the north of San Felipe to Sierra de Guanajuato, juxtaposing Oligocene rocks with the sediments that fill the basin.

The Palo Huérano Fault and La Joya Fault are two NE-SW normal faults with displacements of several tens of meters located in the southeast of the ULRB and are considered part of the Morelia-Acambay system (Martínez-Reyes and Nieto-Samaniego, 1990). Both faults have a length of approximately 20 km and very similar orientations (N50°E), dipping towards the NW and SE respectively. The La Joya Fault was active between 10.6 and 6.2 Ma (Alaniz-Álvarez et al., 2001), while for the Palo Huérano Fault, a fault generation age, before 28.6 Ma, and a reactivation age, after 12.1 Ma, are inferred (Alaniz-Álvarez et al., 2001).

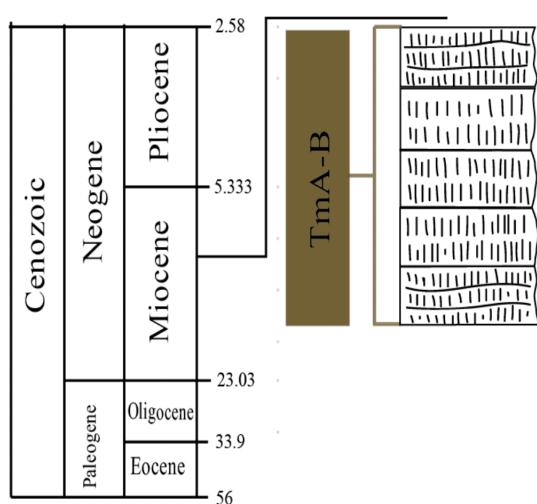
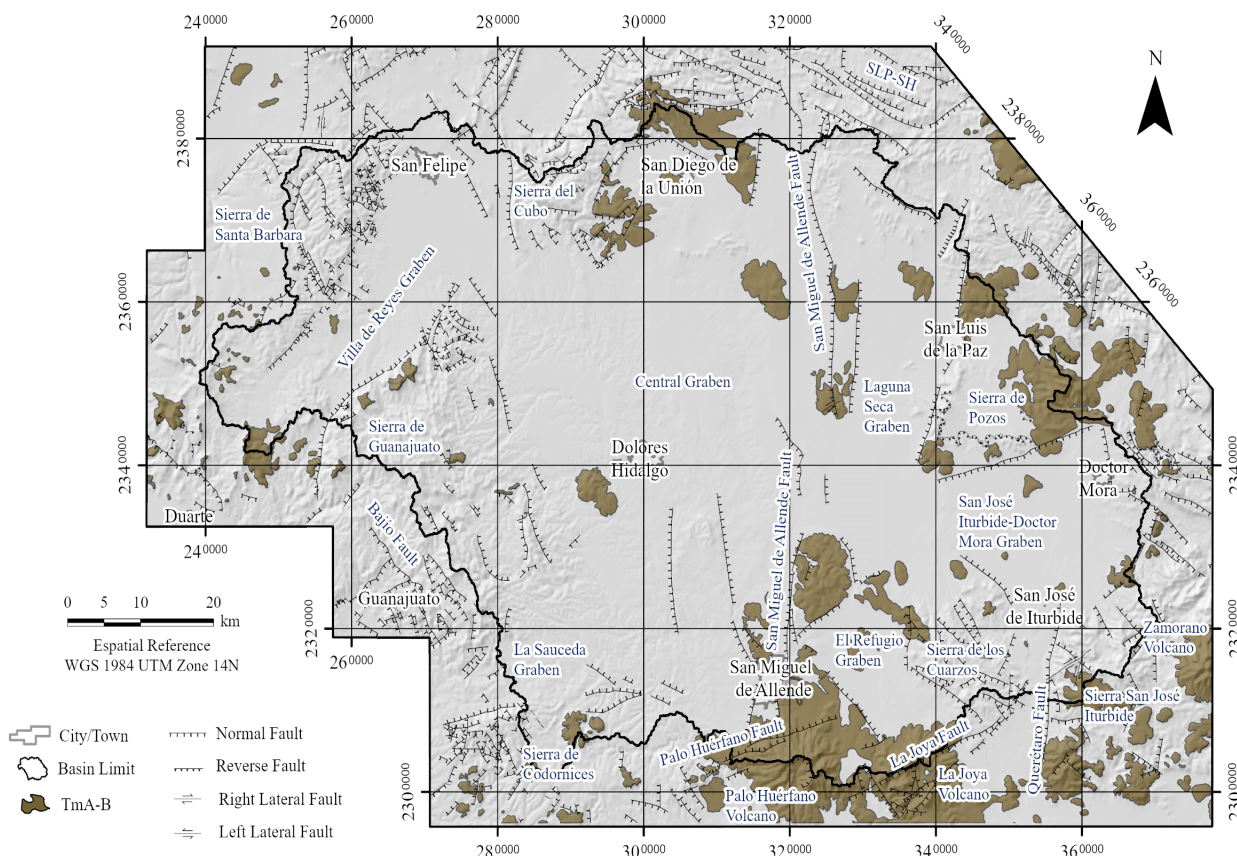
The Bajío Fault System is a NW-SE structure considered the southwestern limit of the Sierra de Guanajuato and Sierra de Codornices (Del Río Varela et al., 2020), with a length greater than 70 km and displacements ranging between 500 and 1,800 m (Hernández-Laloth, 1991; Quintero-Legorreta, 1992). These faults were mainly active during the Eocene and Oligocene, with at least 500 m of displacement occurring after the middle Miocene (Nieto-Samaniego et al., 1999; Alaniz-Álvarez and Nieto-Samaniego, 2005).

The San Luis de la Paz-Salinas Hidalgo Fault System is formed by numerous NW-SE-trending domino faults that were active concurrently with the Villa de Reyes Graben (Labarthe-Hernández and Jiménez-López, 1994). Most of them have southwest dips and can be observed delimiting the northeast of the basin, with lengths ranging from 10 km to 12 km, cutting and displacing Oligocene rocks (Alaniz-Álvarez et al., 2002, Botero-Santa et al., 2020).

## 6. Evolution of main fault systems

The evolution of fault systems during the Eocene-Miocene in some portions of the southern Central Mesa province has been studied by Alaniz-Alvarez et al. (2001), Nieto-Samaniego et al. (2015), Botero-Santa et al. (2015, 2020) and Del Pilar-Martínez et al. (2022). According to these authors, the older deformation event corresponds to the contractile phase of the Laramide Orogeny, which deformed the Jurassic and lower Cretaceous rocks, with an estimated age comprised between the Albian and the Eocene, and a transport direction to the NE (Quintero-Legorreta, 1992).

Between 52 and 49 Ma, the emplacement and exhumation of the Comanja Granite, the deposition of the lower member of the Duarte Conglomerate, the intrusion of the Duarte sill and the emplacement of the La Laborcita Rhyolite were concurrent with a NW-SE transpressional event during the transition between the Laramide shortening and a subsequent extensional event (Angeles-Moreno, 2018).



**Mesa del Obispo basalt:** Basaltic-Andesitic Plateaus  
( $9.6 \pm 0.3$  Ma<sup>B,1</sup>,  $8.7 \pm 0.3$  Ma<sup>B,1</sup>,  $7.6 \pm 0.3$  Ma<sup>B,1</sup>)

**La Joya Volcano:** Basaltic-andesitic lavas.  
( $9.9 \pm 0.4$  Ma<sup>D,5</sup>)

**Zamorano Volcano:** Basaltic-andesitic lavas  
( $10.9 \pm 0.5$  Ma<sup>A</sup>)

**Palo Huérfano Volcano:** Basaltic-andesitic lavas  
( $12.4 \pm 0.3$  Ma<sup>A,2</sup>,  $11.1 \pm 0.4$  Ma<sup>A,4</sup>,  $12.1 \pm 0.6$  Ma<sup>C,4</sup>)

**Mesa de San José basalt:** Basaltic-Andesitic Plateaus  
( $14.8 \pm 0.4$  Ma<sup>A,2</sup>)

Figure 8. Location of Miocene outcrops and Miocene stratigraphic column of the ULRB. Formations included in each chronostratigraphic group are shown according to their reported ages. Dating method: K/Ar in whole rock <sup>A</sup>, K/Ar in rock matrix <sup>B</sup>, K/Ar in plagioclase <sup>C</sup>, Ar/Ar in plagioclase <sup>D</sup>. Source: Ángeles-Moreno (2018)<sup>1</sup>, Cerca-Martínez et al. (2000)<sup>2</sup>, Carrasco-Núñez et al. (1989)<sup>3</sup>, Pérez-Venzor et al. (1996)<sup>4</sup>, Váldez-Moreno et al. (1998)<sup>5</sup> / Figura 8.

Ubicación de los afloramientos del Miocene y columna estratigráfica del Miocene de la CARL. Se muestran las formaciones que incluye cada grupo cronoestratigráfico de acuerdo con sus edades reportadas. Método de datación: K/Ar en roca entera <sup>A</sup>, K/Ar en matriz <sup>B</sup>, K/Ar en plagioclasa <sup>C</sup>, Ar/Ar en plagioclasa <sup>D</sup>. Fuente: Ángeles-Moreno (2018)<sup>1</sup>, Cerca-Martínez et al. (2000)<sup>2</sup>, Carrasco-Núñez et al. (1989)<sup>3</sup>, Pérez-Venzor et al. (1996)<sup>4</sup>, Váldez-Moreno et al. (1998)<sup>5</sup>

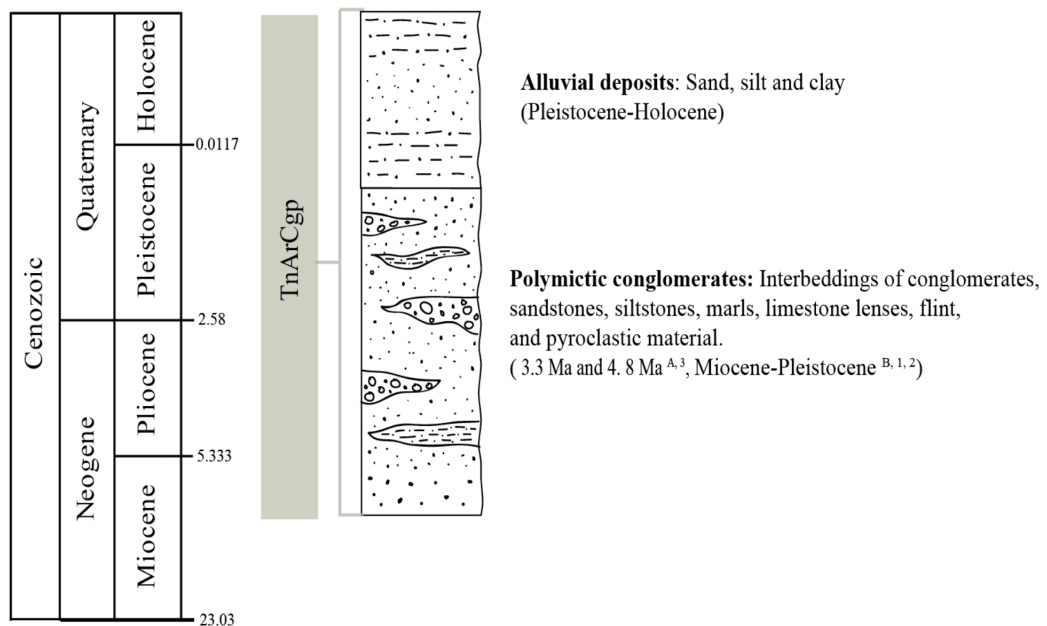
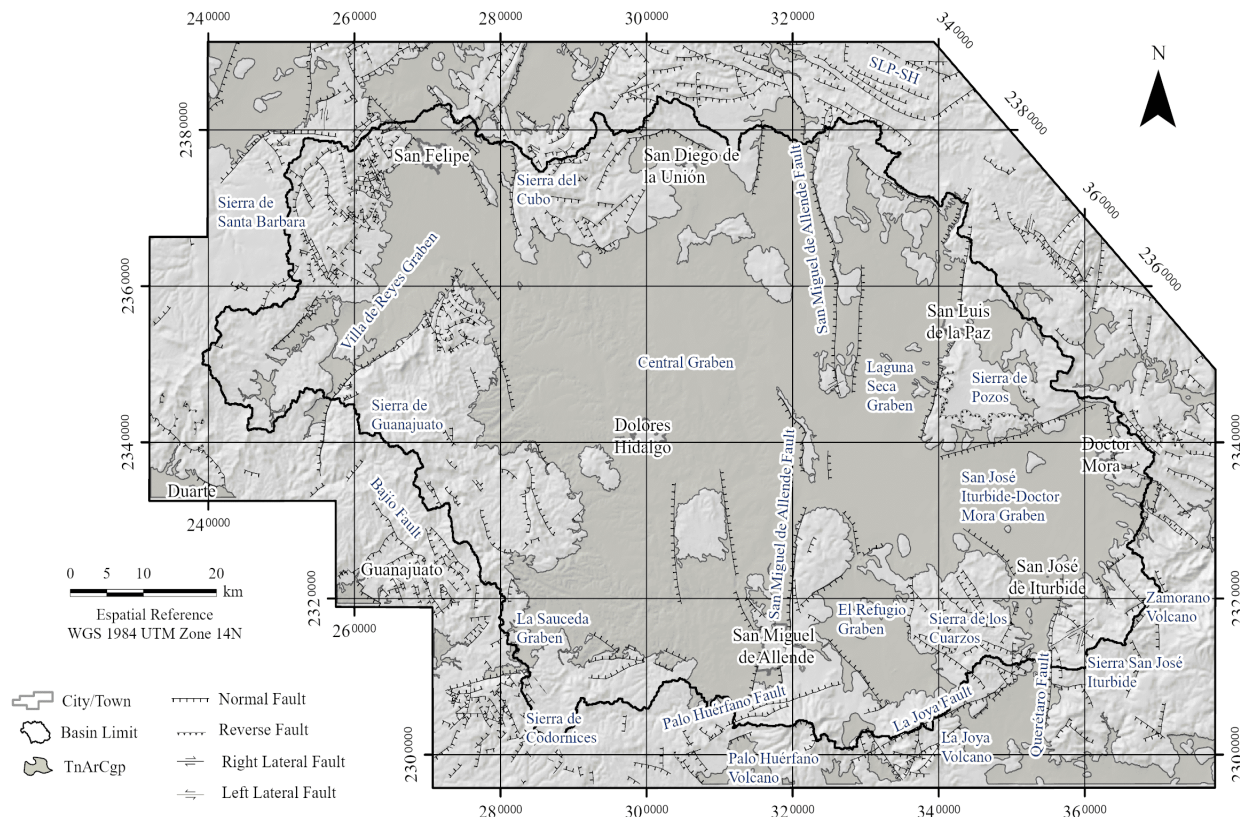


Figure 9. Location of Miocene-Holocene outcrops and Miocene-Holocene stratigraphic column of the ULRB. Formations included in each chronostratigraphic group are shown according to their reported ages. Dating method: Ar-Ar in volcanic ash <sup>A</sup>, Fossil fauna <sup>B</sup>. Source: Carranza-Castañeda et al. (1994)<sup>1</sup>, Miller and Carranza (1998)<sup>2</sup>, Kowallis et al. (1998)<sup>3</sup> / Figura 9. Ubicación de los afloramientos del Miocene-Holoceno y columna estratigráfica del Miocene-Holoceno de la CARL. Se muestran las formaciones que incluye cada grupo crono estratigráfico de acuerdo con sus edades reportadas. Método de datación: Ar-Ar en ceniza volcánica <sup>A</sup>, Fauna fósil <sup>B</sup>. Fuente: Carranza-Castañeda et al. (1994)<sup>1</sup>, Miller and Carranza (1998)<sup>2</sup>, Kowallis et al. (1998)<sup>3</sup>

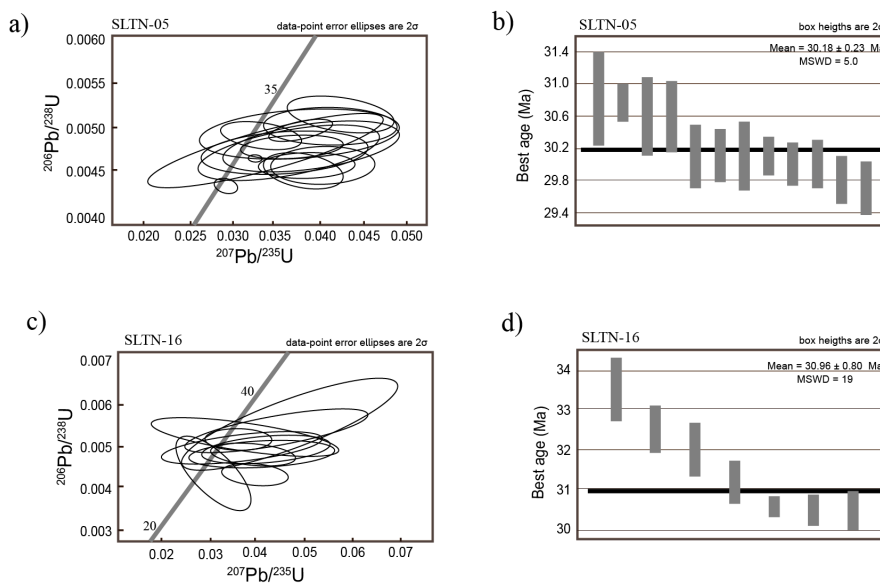


Figure 10. The left image of each sample corresponds to the normal Concordia plots (Wetherill 1956) for the U-Pb isotopic composition of the analyzed zircons. The image on the right shows the weighted average age / Figura 10. La imagen izquierda de cada muestra corresponde a las gráficas normales de Concordia (Wetherill 1956) para la composición isotópica U-Pb de los circones analizados. La imagen de la derecha muestra la edad media ponderada.

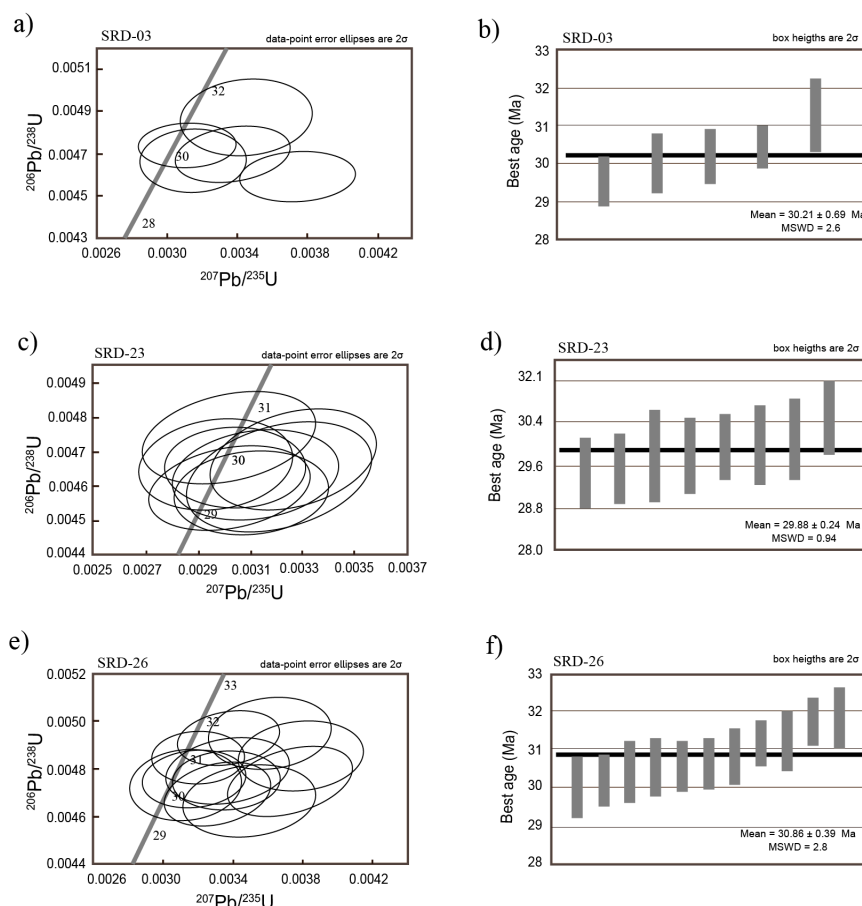


Figure 11. The left image of each sample corresponds to the normal Concordia plots (Wetherill 1956) for the U-Pb isotopic composition of the analyzed zircons. The image on the right shows the weighted average age / Figura 11. La imagen izquierda de cada muestra corresponde a las gráficas normales de Concordia (Wetherill 1956) para la composición isotópica U-Pb de los circones analizados. La imagen de la derecha muestra la edad media ponderada

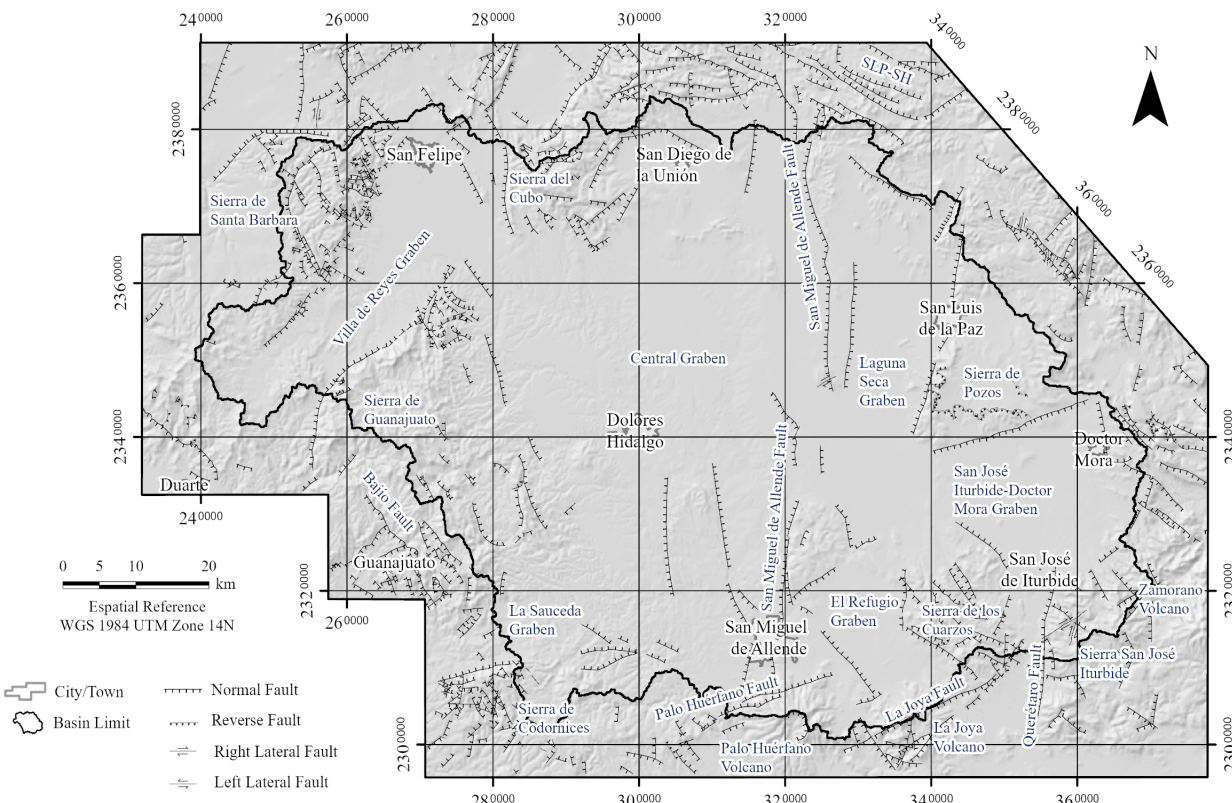


Figure 12. Main structures in Upper Laja River Basin. SLP-SH: San Luis de La Paz-Salinas Hidalgo fault system. The faults were obtained from the geological maps published by the SGM and corrected with the works of Alaniz-Álvarez et al., 2002, Alaniz-Álvarez et al., 2001 and digital elevation models published by INEGI / Figura 12. Principales estructuras de la Cuenca Alta del Río Laja. SLP-SH: Sistema de fallas de San Luis de La Paz-Salinas Hidalgo. Las fallas fueron obtenidas de los mapas geológicos publicados por el SGM y corregidas con los trabajos de Alaniz-Álvarez et al., 2002, Alaniz-Álvarez et al., 2001 y modelos digitales de elevación publicados por el INEGI

Aranda-Gómez and McDowell (1998) proposed another event between 49 and 33 Ma, characterized by extensional deformation, with a NE-SW direction. This event is inferred based on variations in the inclination of the layers and changes in the size of clasts in the upper member of the Guanajuato Conglomerate. This deformation also produced angular unconformities between the Eocene conglomerates and the Oligocene volcanic rocks (Angeles-Moreno, 2018).

Del Pilar-Martínez et al. (2020) interpreted that a biaxial NW trending fault system developed during the Rupelian, forming half-grabens with the master fault on the NE shoulder. The age of this event is estimated at 31 Ma, as an angular unconformity is observed between 31 Ma and 30 Ma volcanic rocks. In the Sierra de Guanajuato, the NW-striking El Bajío Fault was active during this time span, and in the Guanajuato Mining District, Nieto-Samaniego et al. (2016) reported normal faults that tilted 31.5 Ma pyroclastic rocks (Calderones Formation), which were unconformably overlain by 30.5 Ma rhyolites (Chichíndaro Rhyolite). The extensional regime continued with the formation of non-rotational polymodal fault systems that affected middle and late Rupelian rocks, including the

Chichíndaro Rhyolite (Del Pilar-Martínez et al., 2020).

Finally, an extensional deformation phase between 14-6 Ma is registered, which includes two fault sets of NE and NW trends. Is inferred by the faulting affecting andesitic and basaltic plateaus near La Ordeña and the Ignacio Allende dam ( $11.1 \pm 0.4$  Ma, Pérez -Venzor et al., 1996), the Palo Huérfano fault, the NE-SW faults that cut a basaltic plateau to the southeast of La Joya volcano and the reactivation of the Villa de Reyes Graben (Del Pilar-Martínez et al., 2020).

## 7. Conclusions

The geological complexity of the Upper Laja River Basin is a result of the multi-episodic deformation history of the southern part of the Mesa Central province, which has been unraveled in the past decades. However, to achieve a comprehensive and accurate understanding of this basin, an integrative detailed geological-structural map was needed.

Beyond its geological relevance, any basin holds significant hydrological importance, especially in arid regions where they

# Geological Map of the Upper Laja River Basin, Guanajuato, Mexico

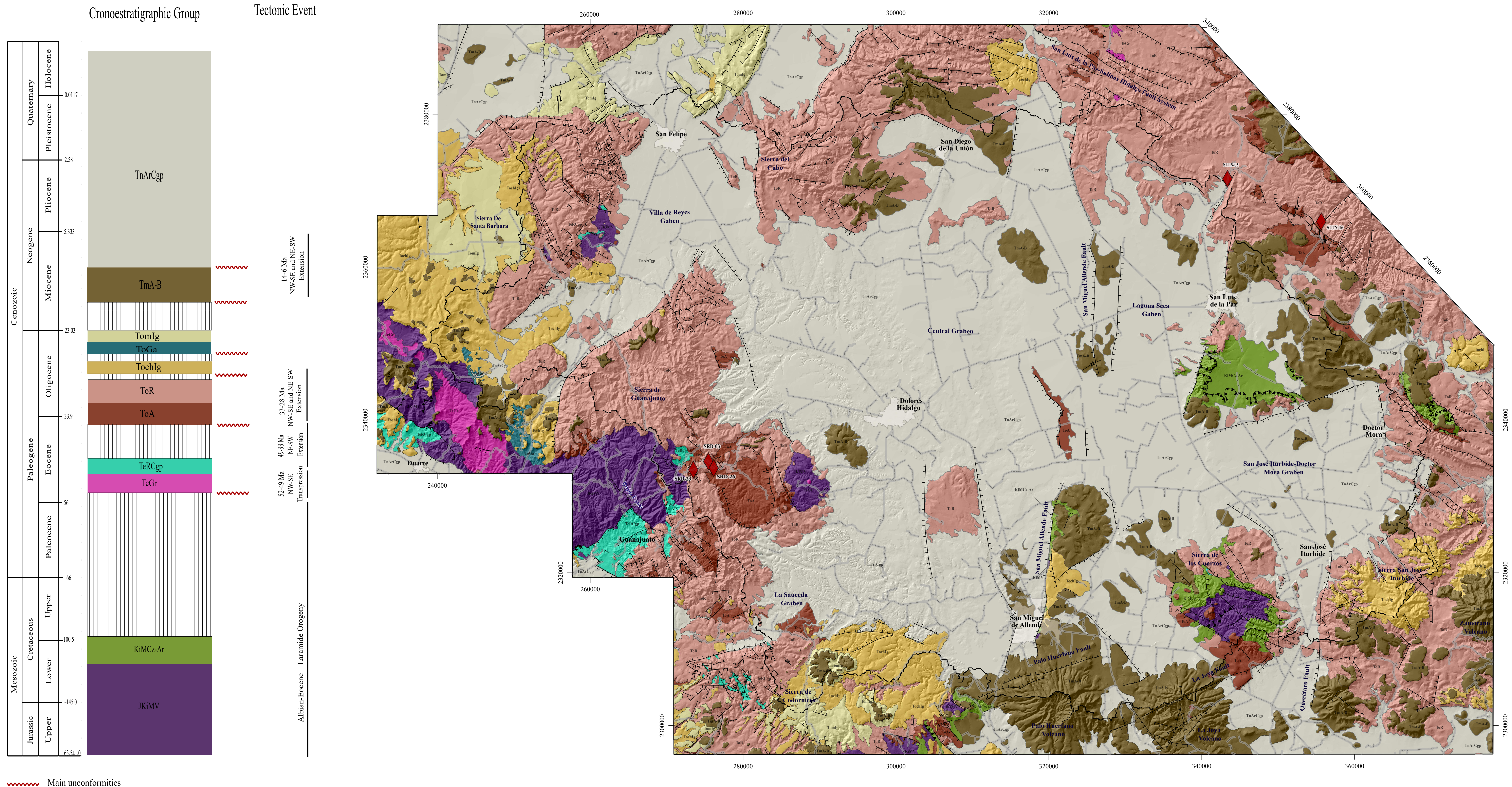
Beatriz Coral Beltrán Martínez<sup>1</sup>, Isidro Loza Aguirre<sup>2</sup>, Yanmei Li<sup>2</sup>, Raúl Miranda Avilés<sup>2</sup>, Ángel F. Nieto Samaniego<sup>3</sup>, Edgar Ángeles Moreno<sup>2</sup>, Pooja Vinod Kshirsagar<sup>2</sup>, María Jesús Puy y Alquiza<sup>2</sup>, Jesús Horacio Hernández Anguiano<sup>4</sup>

<sup>1</sup> Maestría en Ciencias del Agua, División de Ingenierías, Universidad de Guanajuato, 36000, Guanajuato, Gto., México

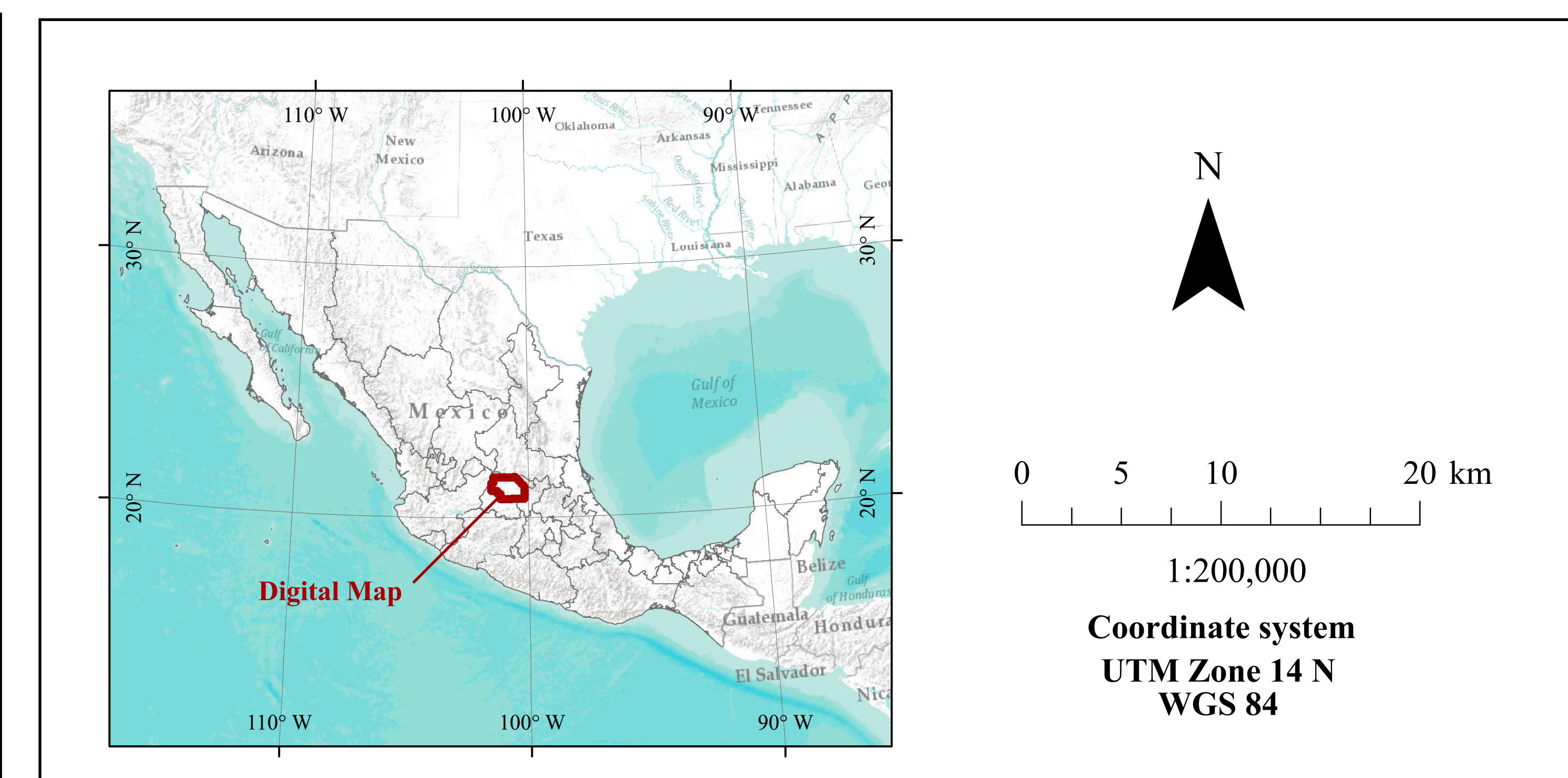
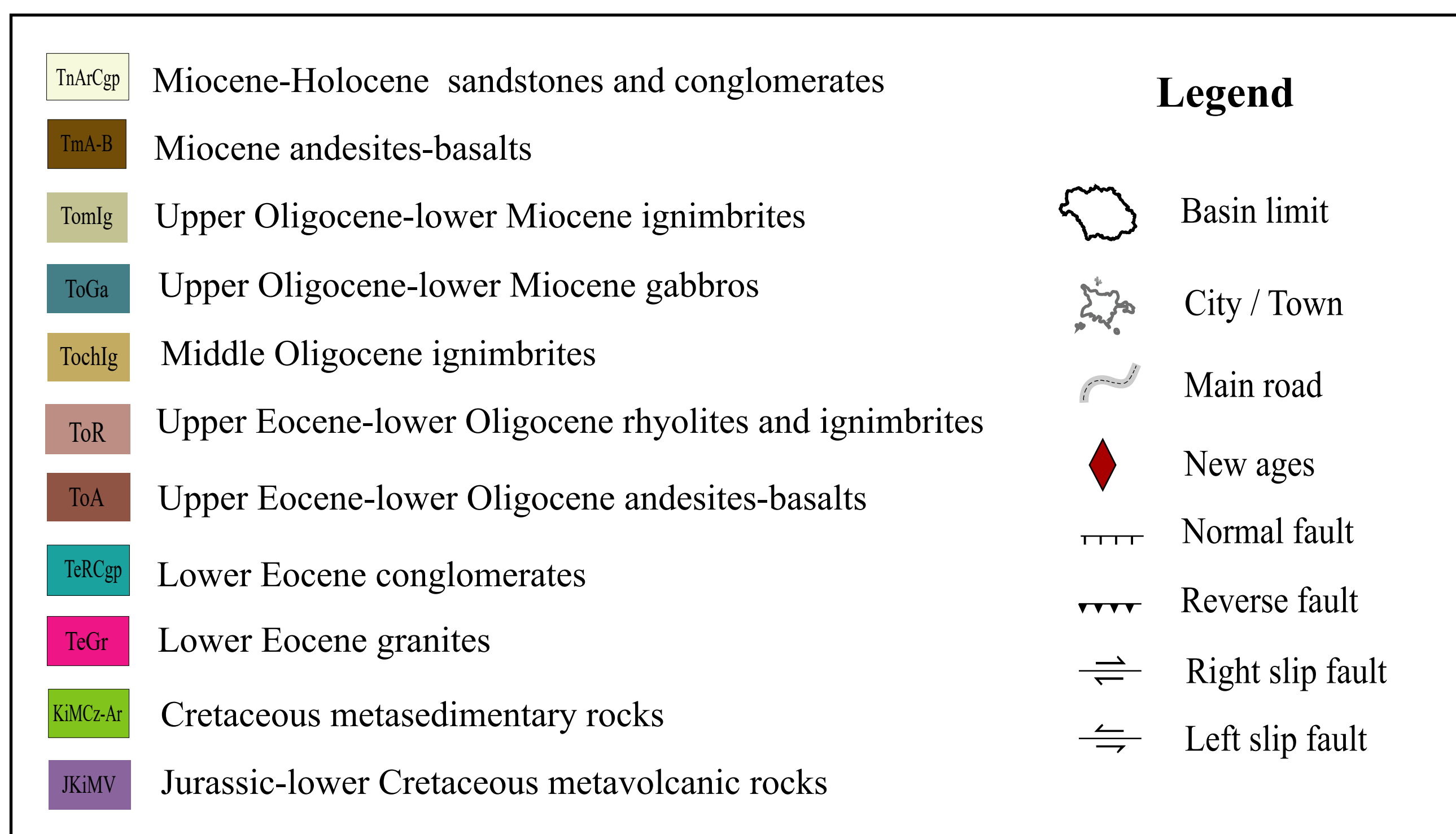
<sup>2</sup> Departamento de Ingeniería en Minas, Metalurgia y Geología, División de Ingenierías, Campus Guanajuato, Universidad de Guanajuato, 36020, Guanajuato, Gto., México

<sup>3</sup> Centro de Geociencias, Universidad Nacional Autónoma de México, Campus Juriquilla, Querétaro, 76230, México

<sup>4</sup> Departamento de Ingeniería Geomática e Hidráulica, División de Ingenierías, Campus Guanajuato, Universidad de Guanajuato, 36000, Guanajuato, Gto., México



>Main unconformities



serve as vital water sources. In this context, the geological conditions of the basin exert a marked influence on multiple aspects of its hydrology, determining the dynamics and behavior of the water resources it holds.

The map of the Upper Laja River Basin presented in this study provides a detailed description of the geology in the area, with stratigraphy categorized into seven main chronostratigraphic groups. Additionally, it identifies the main fault systems that shape and structure the basin. This information is complemented by five new U-Pb ages, which improve the chronostratigraphy of the basin.

The relevance and practical utility of this map are significant, as it offers a solid geological foundation for further studies on water dynamics and sustainable management. This map lays the ground for developing a three-dimensional conceptual hydrogeological model of the basin, enabling a deeper understanding of its internal geologic structure.

## Acknowledgments

To the National Council of Science and Technology (CONACYT) for financing projects 004/2015 and 1013/2016, to YL.

To the financing of project 175/2022, Convocatoria Institucional de Investigación Científica (CIIC) 2022, Universidad de Guanajuato, to ILA.

To Dr. Carlos Ortega-Obregón for the dating carried out in the isotopic studies laboratory, UNAM campus Juriquilla, Querétaro.

BCBM is thankful to the National Council of Science and Technology (CONACYT) for the master's fellowship, whose master's thesis was completed under the supervision of Li Y. and Loza-Aguirre I.

## References

- Alaniz-Alvarez, S. A., Nieto-Samaniego, A. F., Orozco-Esquível, M. T., Vassallo, L. F., Xu, S., 2002. El sistema de fallas Taxco-San Miguel de Allende: Implicaciones en la deformación post-eocénica del centro de México. Boletín de la Sociedad Geológica Mexicana 55 (1), 12–29, <https://doi.org/10.18268/BSGM2002v55n1a2>.
- Alaniz-Alvarez, S. A., Nieto-Samaniego, A. F., Reyes-Zaragoza, M. A., Orozco-Esquível, M. T., Ojeda-García, A. C., 2001. Estratigrafía y deformación extensional en la región San Miguel de Allende-Querétaro, México. Revista Mexicana de Ciencias Geológicas 18 (2), 129–148.
- Alanís-Ruiz, E., 2002. Evolución geológica de la Cuenca de la Independencia y sus alrededores, Estado de Guanajuato, México. Tesis de licenciatura. Universidad Nacional Autónoma de México, Facultad de Ingeniería, México, D.F.
- Alvarado-Méndez, H., López-Ojeda, J. A., Caballero-Martínez, J. A., 1998. Carta Geológico-Minera Guanajuato F14-C43, 1:50,000. Servicio Geológico Mexicano.
- Alvarado-Méndez, H., Rodríguez-Trejo, S., 1999. Carta Geológico-Minera Nuevo Valle de Moreno F14-C42, 1:50,000. Servicio Geológico Mexicano.
- Angeles-Moreno, E., 2018. La evolución tectónica cenozoica de las sierras de Guanajuato y codornices, México. Tesis de doctorado. Universidad Autónoma de México, Centro de Geociencias, Querétaro, México.
- Aranda Gómez, J. J., Henry, C. D., F. Luhr, J., 2000. Evolución tectono-magnética post-paleocénica de la Sierra Madre Occidental y de la porción meridional de la provincia tectónica de Cuencas y Sierras, México. Boletín de la Sociedad Geológica Mexicana 53 (1), 59–71, <https://doi.org/10.18268/BSGM2000v53n1a3>.
- Aranda-Gómez, J. J., McDowell, F. W., 1998. Paleogene Extension in the Southern Basin and Range Province of Mexico: Syndepositional Tilting of Eocene Red Beds and Oligocene Volcanic Rocks in the Guanajuato Mining District. International Geology Review 40 (2), 116–134, <https://doi.org/10.1080/00206819809465201>.
- Arredondo-Mendoza, J. A., García-Ortiz, M., 2007. Carta Geológico-Minera Colón F14-C56, 1:50,000. Servicio Geológico Mexicano.
- Botero-Santa, P. A., Alaniz-Alvarez, S. A., Nieto-Samaniego, A. F., López-Martínez, M., Levresse, G., Shunshan Xu, 2015. Origen y desarrollo de la cuenca El Bajío en el sector central de la Faja Volcánica Transmexicana. Revista Mexicana de Ciencias Geológicas 32 (1), 84–98.
- Botero-Santa, P. A., Xu, S., Nieto-Samaniego, A. F., Alaniz-Alvarez, S. A., 2020. Efecto de las fracturas de enfriamiento en la formación de fallas normales: El ejemplo de Santa María del Río, San Luis Potosí, México. Boletín de la Sociedad Geológica Mexicana 72 (1), 1–23, <https://doi.org/10.18268/BSGM2020v72n011019>.
- Bustos-Gutiérrez, L. A., Romo-Ramírez J. R., 2005. Carta Geológico-Minera San Felipe F14-C33, 1:50,000. Servicio Geológico Mexicano.
- Carranza Castaneda, Oscar, Petersen, M. S., Miller, W. E., 1994. Preliminary investigation of the geology of the northern San Miguel Allende area, north-eastern Guanajuato, Mexico. Geology Studies 40, 1–9.
- Castro-Aceves, J., 2020. Análisis cartográfico y geoquímico en la zona sur de la Mesa Central en el área entre San Luis de la Paz y Tierra Nueva, México. Tesis de licenciatura. Universidad de Guanajuato. Guanajuato, Gto.
- Cerca Martínez, L. M., Aguirre Díaz, G. D. J., López Martínez, M., 2000. The Geologic Evolution of the Southern Sierra de Guanajuato, Mexico: A Documented Example of the Transition from the Sierra Madre Occidental to the Mexican Volcanic Belt. International Geology Review 42 (2), 131–151, <https://doi.org/10.1080/00206810009465073>.
- Chiodi, M., Monod, O., Busnardo, R., Gaspard, D., Sanchez, A., Yta, M., 1988. Une discordance ante albienne datée par une faune d'Ammonites et de Brachiopodes de type téthysien au Mexique central. Geobios 21 (2), 125–135, [https://doi.org/10.1016/S0016-6995\(88\)80014-7](https://doi.org/10.1016/S0016-6995(88)80014-7).
- Davis, J.B., Clark, K. F., Randall, J.A., 2009. Relación de una caldera con la mineralización en el distrito minero de Guanajuato. En: Clark, K.F., Salas Piza, G.A., Cubillas Estrada, R. (Eds.), Geología Económica de México. Servicio Geológico Mexicano y Asociación de Ingenieros de Minas, Metalurgistas y Geólogos de México, pp. 584–635.
- Del Pilar-Martínez, A., Nieto-Samaniego, A. F., Alaniz-Alvarez, S. A., 2020. Development of a Brittle Triaxial Deformation Zone in the Upper Crust: The Case of the Southern Mesa Central of Mexico. Tectonics 39 (11), 1–24, <https://doi.org/10.1029/2020TC006166>.
- Del Pilar-Martínez, A., Nieto-Samaniego, A. F., Angeles Moreno, E., Suárez Arias, A. M., Olmos Moya, M. J. P., Alaniz Alvarez, S. A., Levresse, G., 2021. Digital geological map and geochronological database of the Cenozoic cover of the southern Mesa Central province, Mexico. Terra Digitalis 5 (2), 1–10, <https://doi.org/10.22201/igg.25940694e.2021.2.89>.
- Del Río Varela, P., Nieto-Samaniego, A. F., Alaniz-Alvarez, S. A., Angeles Moreno, E., Escalona-Alcázar, F. D. J., Del Pilar-Martínez, A., 2020. Geología y estructura de las sierras de Guanajuato y Codornices, Mesa Central, México. Boletín de la Sociedad Geológica Mexicana 72 (1), 1–20, <https://doi.org/10.18268/BSGM2020v72n1a071019>.
- Demant, A., 1978. Características del Eje Neovolcánico Transmexicano y sus problemas de interpretación. Revista Mexicana de Ciencias Geológicas 2 (2), 172–187.
- Echegoyén-Sánchez, J., Romero-Martínez, S., Velásquez-Silva, S., 1970. Geología y yacimientos minerales en la parte central del Distrito Minero de Guanajuato. Consejo de Recursos naturales No Renovables Boletín 75, 36.
- Gómez-Ordaz, V., Vázquez-Tortoledo, R., Mejía-Sánchez, J. J., 2016. Carta Geológico-Minera Presa San Bartolo F14-C23, 1:50,000. Servicio Geológico Mexicano.
- Gómez-Ordaz, V., Ávila-Ramos, F. J., 2017a. Carta Geológico-Minera Buenavista F14-C55, 1:50,000. Servicio Geológico Mexicano.

- Gómez-Ordaz, V., Ávila-Ramos, F. J., 2017b. Carta Geológico-Minera Melchor F14-C24, 1:50,000. Servicio Geológico Mexicano.
- Hernández-Laloth, N., 1991. Modelo conceptual de funcionamiento hidrodinámico del sistema acuífero del Valle de León, Guanajuato. Tesis de licenciatura. Universidad Nacional Autónoma de México, Facultad de Ingeniería, México, D.F.
- Kowallis, Bart J., Swisher III, Carl C., Carranza-Castañeda, Oscar, Miller, Wade E., Tingey, David G., 1998. Fission-track and single-crystal 40Ar/39Ar laser-fusion ages from volcanic ash layers in fossil-bearing Pliocene sediments in central Mexico. *Revista Mexicana de Ciencias Geológicas* 15 (2), 157–160.
- Labarthe-Hernández, G., Tristán ,G. M., 1978. Cartografía Geológica de la Hoja San Luis Potosí, Universidad Autónoma de San Luis Potosí, Instituto de Geología y Metalurgia, Folleto técnico 59.
- Labarthe-Hernández, G., Tristán ,G. M., Aranda-Gómez, J. J., 1982. Revisión estratigráfica del Cenozoico de la parte central del estado de San Luis Potosí. Universidad Autónoma de San Luis Potosí, Instituto de Geología y Metalurgia, Folleto técnico (Open-File Report) 85.
- Lemos-Bustos, O., Flores-Salas, J. J., 2020. Carta Geológico-Minera Sierra de Jacales F14-C22, 1:50,000. Servicio Geológico Mexicano.
- Ludwig, K. L., 2008. Isoplot 3.7. A geochronological toolkit for Microsoft Excel. Berkeley Geochronology Center Special Publication.
- López-Ojeda, J. A., Loaeza-García, J. P., Zárate-Barradas, R., 2002. Carta Geológico-Minera Aldama F14-C53, 1:50,000. Servicio Geológico Mexicano.
- Martini, M., Mori, L., Solari, L., Centeno-García, E., 2011. Sandstone Provenance of the Arperos Basin (Sierra de Guanajuato, Central Mexico): Late Jurassic-Early Cretaceous Back-Arc Spreading as the Foundation of the Guerrero Terrane. *The Journal of Geology* 119 (6), 597–617, <https://doi.org/10.1086/661989>.
- Martínez-Reyes, J., 1992. Mapa geológico de la Sierra de Guanajuato, con resumen de la geología de la Sierra de Guanajuato. Cartas geológicas y mineras 8. Mapa de escala 1: 100,000 con texto explicativo en el reverso. Universidad Nacional Autónoma de México, Instituto de Geología. Servicio Geológico Mexicano.
- Martínez-Reyes, J., Nieto-Samaniego, Angel Francisco, 1990. Efectos geológicos de la tectónica reciente en la parte central de México. *Revista Mexicana de Ciencias Geológicas* 9 (1), 33–50.
- Miller, Wade E., Carranza-Castañeda, Oscar, 1998. Importance of late Tertiary carnivores and equids from the Transmexican Volcanic Belt. *Revista Mexicana de Ciencias Geológicas* 15 (2), 161–166.
- Monod, O., Lapierre, H., Chiodi, M., Martinez, J., Calvet, P., Ortiz, E., Zimmerman, J. L., 1990. Reconstitution d'un arc insulaire intra-océanique au Mexique central: la séquence volcano-plutonique de Guanajuato (Crétacé inférieur). *Comptes Rendus de l'Académie des Sciences de Paris* 310 (1), 45–51.
- Nieto Samaniego, A. F., 2012. Geología de la región de Salamanca, Guanajuato, México. Boletín de la Sociedad Geológica Mexicana 64 (3), 411–425, <https://doi.org/10.18268/BSGM2012V64n3a10>.
- Nieto-Samaniego, A. F., Báez-López, J. A., Levresse, G., Alaniz-Alvarez, S. A., Ortega-Obregón, C., López-Martínez, M., Nogués-Alcántara, B., Solé-Viñas, J., 2016. New stratigraphic, geochronological, and structural data from the southern Guanajuato Mining District, México: implications for the caldera hypothesis. *International Geology Review* 58 (2), 246–262, <https://doi.org/10.1130/00206814.2015.1072745>.
- Nieto-Samaniego, A. F., Ferrari, L., Alaniz-Alvarez, S. A., Labarthe-Hernández, G., Rosas-Elguera, J., 1999. Variation of Cenozoic extension and volcanism across the southern Sierra Madre Occidental volcanic province, Mexico. *GSA Bulletin* 111 (3), 347–363, [https://doi.org/10.1130/0016-7606\(1999\)111<0347:VOCEAV>2.3.CO;2](https://doi.org/10.1130/0016-7606(1999)111<0347:VOCEAV>2.3.CO;2).
- Nieto-Samaniego, Angel Francisco, 1990. Fallamiento y estratigrafía cenozoicos en la parte sudoriental de la Sierra de Guanajuato. Universidad Nacional Autónoma de México, Instituto de Geología, Revista 9 (2), 146–155.
- Nieto-Samaniego, Angel Francisco, Alaniz-Alvarez, Susana Alicia, Cerca-Martínez, M., Reyes-Zaragoza, M. A., Concha-Dimas, A., 1999. Carta Geológico-Minera San Miguel de Allende F14-C54, 1:50,000. Servicio Geológico Mexicano.
- Nieto-Samaniego, Angel Francisco, Alaniz-Alvarez, Susana Alicia, Labarthe-Hernández, Guillermo, 1997. The post-Laramide Cenozoic deformation in the southern mesa Central, Mexico. *Revista Mexicana de Ciencias Geológicas* 14 (1), 13–25.
- Nieto-Samaniego, Angel Francisco, García-Dobarganes Bueno, Juan Esteban, Aguirre-Maese, Ana Laura, 1992. Interpretación estructural de los rasgos geomorfológicos principales de la Sierra de Guanajuato. *Revista Mexicana de Ciencias Geológicas* 10 (1), 1–5.
- Nieto-Samaniego, Angel Francisco, Macías-Romo, Consuelo, Alaniz-Alvarez, Susana Alicia, 1996. NOTA CORTA - Nuevas edades isotópicas de la cubierta volcánica cenozoica de la parte meridional de la Mesa Central, México. *Revista Mexicana de Ciencias Geológicas* 13 (1), 117–122.
- Ortiz-Hernández, Luis Enrique, Chiodi , Michel, Lapierre , Henriette, Monod, Olivér, Calvet, Philippe, 1990. El arco intraoceánico alóctono (Cretácico Inferior) de Guanajuato-características petrográficas, geoquímicas, estructurales e isotópicas del complejo filoniano y de las lavas basálticas asociadas—implicaciones geodinámicas. *Revista Mexicana de Ciencias Geológicas* 9 (2), 126–145.
- Procesos Analíticos Informáticos S.A. de C.V., 2008a. Carta Geológico-Minera San Diego de la Unión F14-C34, 1:50,000. Servicio Geológico Mexicano.
- Procesos Analíticos Informáticos S.A. de C.V., 2008b. Carta Geológico-Minera San Luis de la Paz F14-C35, 1:50,000. Servicio Geológico Mexicano.
- Pérez-Vargas, M. A., López-Ojeda, J. A., Alvarado-Méndez, H., Saldaña-Saucedo, G., 1996. Carta Geológico-Minera Dolores Hidalgo F14-C44, 1:50,000. Servicio Geológico Mexicano.
- Pérez-Venzor, José Antonio, Aranda-Gómez, José Jorge, McDowell, Fred, Solorio-Munguía, José Gregorio, 174. Geología del volcán Palo Huérfano, Guanajuato, México. *Revista Mexicana de Ciencias Geológicas* 13 (2).
- Quintero Legorreta, O., 1992. Geología de la región de Comanja, Estados de Guanajuato y Jalisco. *Revista mexicana de ciencias geológicas* 10 (1), 6–25.
- Reyes-Reyes, N. A., Luna-Castro, H., 1998. Carta Geológico-Minera Mineral de Pozos F14-C45, 1:50,000. Servicio Geológico Mexicano.
- Ruiz-González, F., 2015. Estudio de las vetas de turmalina que registran la historia de exhumación del Granito Comanja, Sierra de Guanajuato, México. Tesis de maestría. Universidad Nacional Autónoma de México, Posgrado en Ciencias de la Tierra.
- Servicios Geológicos Mineros S.A. de C.V., 1999a. Carta Geológico-Minera Doctor Mora F14-C46, 1:50,000. Servicio Geológico Mexicano.
- Servicios Geológicos Mineros S.A. de C.V., 1999b. Carta Geológico-Minera Tierra Nueva F14-C25, 1:50,000. Servicio Geológico Mexicano.
- Servicios Geológicos Mineros S.A. de C.V., 2001. Carta Geológico-Minera Xichú F14-C36, 1:50,000. Servicio Geológico Mexicano.
- Solari, L. A., González-León, C. M., Ortega-Obregón, C., Valencia-Moreno, M., Rascón-Heimpel, M. A., 2018. The Proterozoic of NW Mexico revisited: U-Pb geochronology and Hf isotopes of Sonoran rocks and their tectonic implications. *International Journal of Earth Sciences* 107 (3), 845–861, <https://doi.org/10.1007/s00531-017-1517-2>.
- Soto-Araiza, R. G., Arredondo, J. A., 2005. Carta Geológico-Minera Ibarra F14-C32, 1:50,000. Servicio Geológico Mexicano.
- Tristán-González, M., 1986. Estratigrafía y Tectónica del Graben de Villa de Reyes en los Estados de San Luis Potosí y Guanajuato, México. Folleto Técnico 107. Universidad Autónoma de San Luis Potosí, Instituto Geología.
- Valdés-Moreno, Gabriel, Aguirre-Díaz, Gerardo de Jesús, López-Martínez, Margarita, 1998. El volcán La Joya, Estados de Querétaro y Guanajuato: un estrato volcán miocénico del Cinturón Volcánico Mexicano. *Revista Mexicana de Ciencias Geológicas* 15 (2), 181–197.
- Vassallo, L., Flores, L., Lazcano, L. M., Hernández, G., Solorio, G., Maples, M., Girón, P., Garduño, C., 2001. El gabro de Arperos y su aportación de Cr-Ni a la subcuenca del río Silao, Guanajuato, México. *Ingeniería hidráulica en México* (1985) 16 (1), 63–72.

**This article accompanies the following material:**

Static map: [10.22201/igg.25940694e.2023.2.104.233](https://doi.org/10.22201/igg.25940694e.2023.2.104.233)

Interactive map: [10.22201/igg.25940694e.2023.2.104.234](https://doi.org/10.22201/igg.25940694e.2023.2.104.234)